



Application of titanium dioxide for the photocatalytic degradation of macro- and micro-plastics: A review

Iqra Nabi^a, Aziz-Ur-Rahim Bacha^{a,*}, Farhad Ahmad^a, Liwu Zhang^{a,b,**}

^a Department of Environmental Science and Engineering, Fudan University, Shanghai 200433, People's Republic of China

^b Shanghai Institute of Pollution Control and Ecological Security, Shanghai 200092, People's Republic of China

ARTICLE INFO

Editor: Dr. G. Palmisano

Keywords:

Plastics
TiO₂ application
Plastics degradation
Mechanism
TiO₂ synthesis

ABSTRACT

The advancement in industries and modern technology has been escorted by an expansion in the utilization of chemicals to obtain plastic-based products. Increased plastic production and disposal have greatly affected the environment and living organisms globally. Macro and micro-plastics have a persistent nature, and their natural degradation takes years. Transport, impact, behavior, and degradation have attracted growing research attention. However, a review study on titanium dioxide (TiO₂) based photocatalytic degradation of macro and micro-plastics has not been summarized. Herein, a brief overview of the TiO₂ application for macro and micro-plastics degradation has been summarized. Different preparation methods for TiO₂ synthesis and its modification for plastics decomposition have been presented. The degradation efficiency and applied system limitations with future research directions are proposed. Nevertheless, the existing knowledge about the TiO₂ application for macro and micro-plastics is still limited. This work provides a good reference for plastic pollution control.

1. Introduction

Environmental contamination, devastation, and the need for sufficient clean air and water are serious issues that the world is confronted with. Meanwhile, the rapid increase in world population, pervasive unregulated accelerated energy consumption, and plastics production (more than 90% of total world production) [1] have all contributed to industrial expansion. Whereas the unabated discharge of harmful contaminants and waste into the environment has resulted in major environmental issues such as global warming, water, and air pollution [2]. Plastics production and its use are estimated to expand over the coming days, and more than three hundred kinds of plastics are manufactured in which more than sixty types of plastics are popular [3]. Million tons of plastics and plastic-based material have been manufactured since the middle of preceding era, with more than two hundred million tons of production per annum. E.J. carpenter first time reported plastic pellets' alarm sound in the north Atlantic Ocean, while their focus was on communities studying small plastic pollution [4]. Still, speculation remains how much plastic and debris will reach the oceans, rivers, seas, and landfill sites where it undergoes decomposition and fragmentation [5]. Microplastics (MPs) are further disintegrated into nano plastic

particles following their ingestion by organisms, affecting excretion, metabolism, digestion, and reproduction. In order to control MPs pollution, it is crucial to not only consider the MPs source but also need to focus on transportation and possible solution in the environment [6]. MPs have been found in different environments such as soil, and water [7]. Major MPs transport route from various sources to environmental media is depicted in Fig. 1. Atmospheric fluxes are a vital component of the universal cycle of different elements. While these fluxes are caused due to the transport of elements from distant emission sources to receptor areas [8]. Microplastics (particles with a size less than 5 mm) can proliferate, transport, and accrue in the environment. MPs deposits on beaches, sea surface, sea bed, sand, and sediments [9–11]. Most plastics are intended for a single-use application and applied to mulch film and greenhouse material in developing countries [3]. According to United Nations Environment Programme (UNEP), a huge amount of modern plastic manufacturing has shifted toward single-use plastics [12].

Generally, plastics are prepared from oils, and plastics production consumes approximately 1.6 billion liters of oil annually [13]. The term "plastics" incorporates materials composed of different components such as hydrogen, carbon, nitrogen, oxygen, sulfur, and chlorine. Most prevalent plastics include PE, PP, PVC, PS, PU, and phenolic resin with

* Corresponding author.

** Corresponding author at: Department of Environmental Science and Engineering, Fudan University, Shanghai 200433, People's Republic of China.

E-mail addresses: urbaziz17@fudan.edu.cn (A.-U.-R. Bacha), zhanglw@fudan.edu.cn (L. Zhang).

PP and PE being the most commonly used plastics in daily life [3] while the small quantity of polysulfone, polycarbonate, PLA, and acrylonitrile butadiene styrene copolymer has also been reported [14]. The chemical structure of commonly used plastics with the amount of produced waste is shown in Fig. 2a. Plastics can be divided into two types such as homo-chain plastics (C-C bond in the main chain like PS, PP, PE, etc.) and hetero-chain plastics (different bonds in the main chain like PET, PA, etc.) [15]. Degradation of homo-chain plastics involves three steps such as initiation (bond breakage takes place through light leading to reactive species formation), propagation (ultimate chain scission and cross-linking), and termination (reaction completion) under natural environmental condition. Although, hetero-chain plastics undergo photodegradation, biodegradation, and hydrolysis which causes deterioration in the aquatic environment. The brief photocatalytic degradation pathway of plastics produces several intermediates such as long alkanes/olefins chain, small molecules acid, CH_3COOH , and hydrogen leading to their mineralization [14]. However, most of the single time used plastics end up in the form of mismanaged waste leading to the loss of valued resources [16,17]. Accumulated plastic waste shows an adverse effect on living organisms and the environment [18,19]. Plastics means malleable, which can be changed into any shape [20] and exhibits a high level of thermal and electrical insulation standards [10]. Probable risks linked with plastic cannot be generalized as MPs and nano-plastics (NPs) encompass a heterogeneous group of particles that are different in composition, additive concentration, shape, size, and physicochemical characteristics. Plastics can be categorized into different classes based on their size. Mega plastics have a size $> 1 \text{ m}$, macroplastic ($> 2.5 \text{ cm}$), mesoplastics ($> 5 \text{ mm}$), microplastic ($< 5 \text{ mm}$) and nano-plastic ($< 1 \mu\text{m}$) [21,22]. There are many unsolved questions about MPs in the aquatic media, including the basic question about the amount of MPs [23]. MPs and NPs are a cause of concern due to their following features that are linked with their small particle size: (1) they can transfer rapidly in the environment; (2) have high surface area for contaminants adsorption; (3) can easily move and transfer in the food web, and (4) could transfer to animals [24]. MPs can be divided into primary and secondary plastics based on their sources [24,25]. Primary MPs are discharged in the form of beads, pellets, fibers, and other forms. In contrast, secondary MPs are produced from bigger plastics due to their biological, physical, and chemical actions.

Generally, a major portion of MPs is produced from the breakdown of large plastics due to the action of heat, light, oxidation, and microbes [26].

Titanium dioxide (TiO_2) often recognized as titanium (IV) oxide, belongs to the transition metals oxides family and has been used in numerous applications such as cosmetic products, sunscreens [27], photovoltaic cell [28], environmental remediation [29], nano paint [30], and antibacterial agent [31]. Several other environmentally friendly materials such as nickel nanowires [32–34], nickel nanopillars [35], and bismuth [36–39] have been used for environmental applications but these materials have not been tested for plastics decomposition. TiO_2 is considered a vital photocatalyst that mainly works under the UV region [40]. It has been used in different applications for decades and is documented as a safe and inert photocatalytic material [41]. It plays an effective role in pollutant oxidation during photocatalytic degradation reactions [42]. It is a low-cost commonly used semi-conducting material that can be easily prepared at lab scale [43,44]. Notably, this white pigment material is used since ancient times, which proved it a safe material for humans and the environment [40,45]. Generally, two kinds of photochemical reactions occur on TiO_2 upon light irradiation. One incorporates the light-induced redox reactions of adsorbed materials, while other involves the light-induced hydrophilic conversion of TiO_2 . These combinations open new avenues for the novel application of TiO_2 , especially in the building materials discipline [46]. TiO_2 has been used for different kinds of pollutants decomposition such as persistent pollutants [38], azo dyes [47], and emerging contaminants [48]. Simultaneously, scientists also used TiO_2 for the decomposition of macro and micron size plastics. Though, N modified TiO_2 was firstly employed for commercial MPs HDPE degradation in 2019 [49]. Meanwhile, researchers made a lot of attempts to develop TiO_2 photocatalyst for different types of MPs decomposition. Timeline for the development of various modified TiO_2 for photocatalytic degradation of MPs with their degradation efficiency is shown in Fig. 2b. To our knowledge, there is no review report on TiO_2 application for plastics degradation. The intention of this work to fill the present space in literature. A report of this nature is essential and vital to keep the discipline going forward.

This study aims to present a comprehensive overview of TiO_2 preparation methods, main characteristics, and current progress in the application for dealing with plastics pollution. It highlights the primary

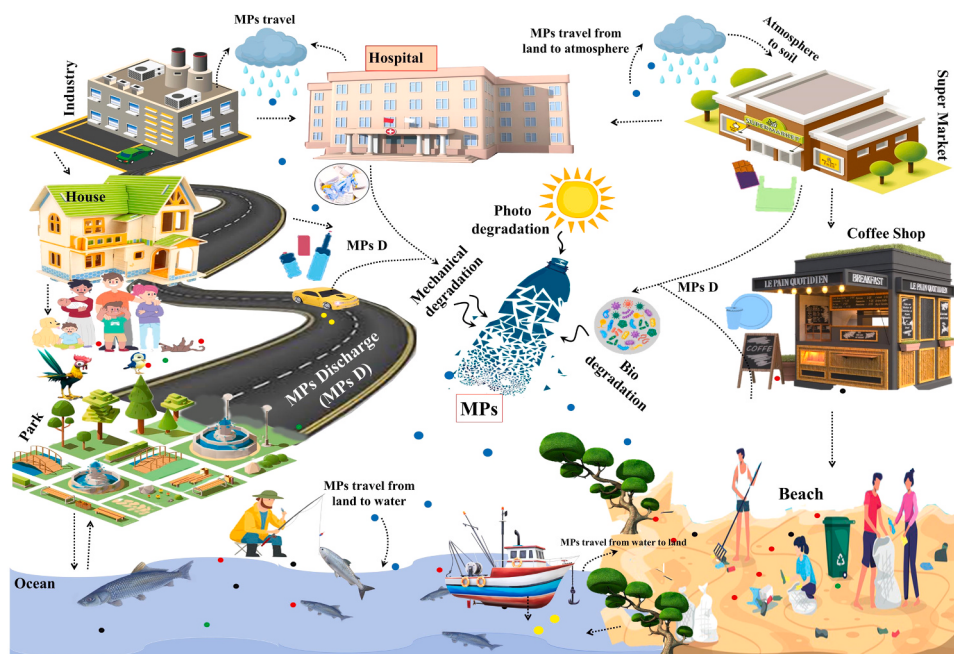


Fig. 1. Major sources and transport routes of MPs in the environment.

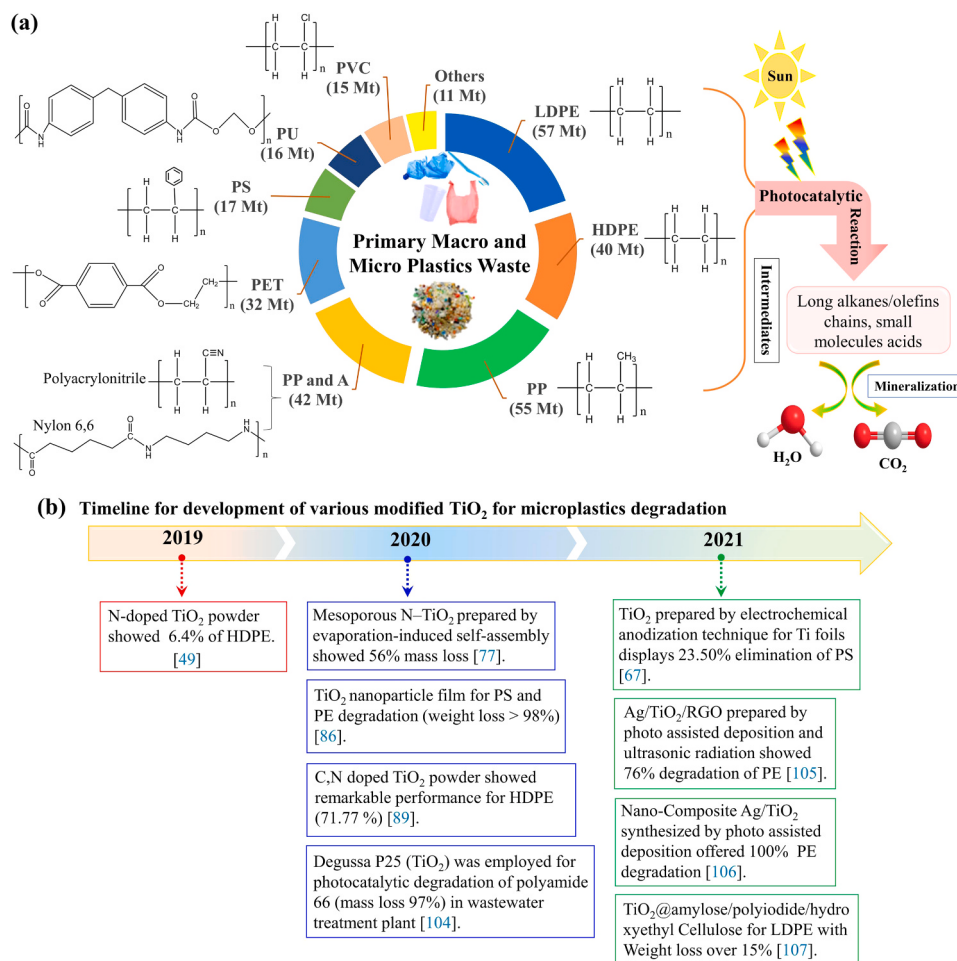


Fig. 2. (a) Common used plastics with their chemical structure and photocatalytic degradation strategy. (Here: Mt indicates metric tons unit). (b) Timeline for the development of TiO₂ for MPs degradation.

mechanism of TiO₂ with structural modification over time. Moreover, it also offers a detailed analysis of reported works on TiO₂ and gives us a better overview of potential developments in TiO₂ for macro and micro-plastics degradation. The main objective is to investigate the performance of TiO₂ for plastics decomposition and also suggest limitations with future research direction. Description of the fact/procedure was to summarize all used synthesis methods for TiO₂ especially for macro and micro-plastics degradation. We believe this work will help researchers to synthesize and improve the performance of TiO₂ for dealing with plastics and emerging contaminants.

2. Literature review

Recently, plastics have gained much research attention due to their adverse health effect and environmental impact. Scientific journals relating to macro and micro-plastics treatment, photocatalysis, and TiO₂ were thoroughly assessed in order to select the relevant results and content for this review. A similar thing was done by using Google Scholar, Elsevier, and Springer link. The keywords include TiO₂, plastics, MPs, and modified TiO₂. For the purpose of data collection, numerous studies were scrutinized.

3. Mechanism of TiO₂ for plastic degradation

The energy bandgap between the conduction (CB) and valence (VB) band of TiO₂ is small. VB electron becomes excited and moves to CB upon light irradiation that is typically in UV A spectrum (315–400 nm)

[50]. Electron (e^-) may move to or from the adsorbent, which forms the positive or negative charged species [51]. Generally, anatase TiO₂ has a large bandgap of 3.2 eV which corresponds to excitation wavelength 388 nm and allows it to absorb light near the UV region. Rutile TiO₂ exhibits a 3.0 eV bandgap which absorbs visible light with a wavelength of 410 nm [52]. The excitation and subsequent transfer process of TiO₂ to CB are shown in Fig. 3a. There are two basic principles or mechanism that takes part in plastics degradation.

3.1. Indirect degradation

Indirect photocatalytic degradation of plastics can be summarized into the following steps:

3.1.1. Excitation

The photocatalytic reaction begins when the electron from the VB is promoted toward the empty CB upon light irradiation [53]. The incident photon has either equal or greater energy than the bandgap of TiO₂. This excitation leaves the holes (h^+) in the VB and the reaction upon light irradiation is summarized in Eq. (1):



3.1.2. Water ionization

A hole in the VB reacts with a water molecule that produces hydroxyl radical ($\cdot\text{OH}$) according to the following Eq. (2). $\cdot\text{OH}$ radical is a strong oxidizing agent that plays an important role in photooxidation [54,55].

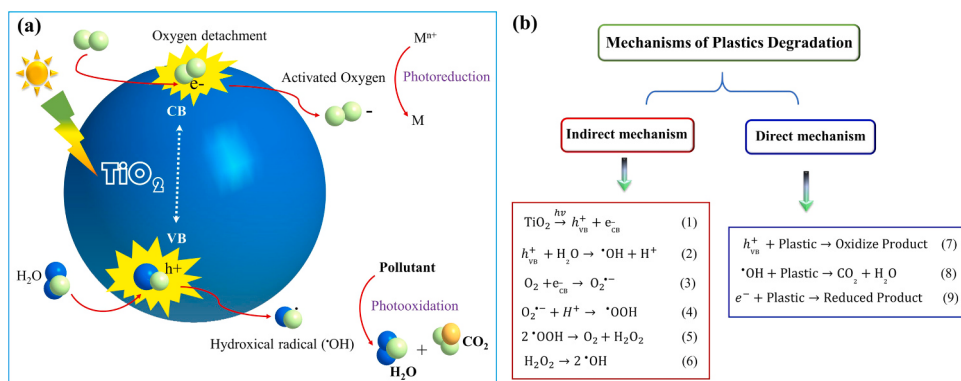


Fig. 3. (a) General photocatalytic mechanism of TiO_2 under light irradiation. (b) Overall photocatalytic mechanism of TiO_2 for plastics decomposition under light irradiation.

It attacks adsorbed contaminant non selectively that is attached or near to the photocatalyst interface surface, leading to its mineralization [56]. TiO_2 is useful for the photodegradation of organic pollutants under UV and visible light [57].



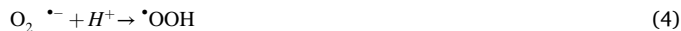
3.1.3. Superoxide radical's formation

Photoexcited electron in the CB reacts with oxygen molecule leading to the generation of superoxide radical (O_2^\bullet) in accordance with Eq. (3) [58]. This O_2^\bullet radical take part in oxidation while also preventing the recombination of photogenerated electron-hole pairs, hence sustaining electron neutrality with semiconductor [59].



3.1.4. Superoxide protonation

Produced O_2^\bullet radical protonated to form hydroperoxyl radical (HO_2^\bullet), as shown in Eq. (4), which further forms hydrogen peroxide (H_2O_2) (Eq. (5)). H_2O_2 further dissociate to produce the $\cdot\text{OH}$, according to Eq. (6).



3.1.5. Overall reaction

For better understanding, the overall reaction for plastics degradation is shown in the following Eqs. (7)–(9).



3.2. Direct degradation

Direct degradation of plastics by TiO_2 also takes place to some extent under visible light. It involves the excitation of plastics from the ground state to the excited state upon visible light photon incident. This excited state of plastics forms semi-oxidized cation radicals through e^- injection in CB of catalyst. Trapped electrons react with dissolved oxygen leading to the formation of O_2^\bullet which subsequently forms $\cdot\text{OH}$ that is responsible for target pollutant decomposition [59–61].



The indirect mechanism of plastics degradation dominates over the direct mechanism, and plastic decomposition is more noticeable than visible-light-induced reaction. Additionally, the visible-light-induced reactions are much slower as compared to UV light-based reactions. The direct and indirect mechanisms for plastics degradation are presented in Fig. 3b.

4. Fabrication of TiO_2 material for plastics degradation

The nature of catalytic material plays an essential role in the photodegradation of plastics. Meanwhile, arrays of preparation methods are present to synthesize pure, modified, doped, and nano TiO_2 . Photocatalytic material should have the capacity to harvest a substantial portion of the light spectrum. The preparation of each method for catalyst fabrication is summarized below:

4.1. Sol-Gel TiO_2

Sol-gel method is also known as chemical solution deposition [62], which is considered an important method for the preparation of TiO_2 . Typically, sol is formed by hydrolysis and polycondensation reactions of precursor solution [63]. The process for obtaining the sol-gel TiO_2 powder includes four steps. Initially, 10 mL titanium isopropoxide (TTIP) was mixed in 500 mL ethanol and refluxed overnight. Secondly, aqueous citrate solution (0.5 M) was poured drop by drop in the refluxed solution following 24 h mechanical stirring, leading to gel formation. Fourthly, the obtained gel was dried for a week in room condition. The dried powder was grounded in a mortar and finally calcined in a muffle furnace at 400 °C for 1 h and 30 min [64].

The second method for sol-gel TiO_2 powder preparation for polyethylene (PE) degradation is as fellow: Tetra butyl titanate (Ti(OBu)_4) was mixed in 34 mL ethanol under stir for 5 min following the addition of 2 mL diethanolamine (DEA). The solution was kept for 1 h stir (named solution-A). Solution-B consist of deionized (DI) water (0.5 mL) and ethanol (5 mL), which was added dropwise in solution-A within 30 min. The obtained solution was hydrolyzed at room condition until it turns light yellow, succeeding the aging at room condition for 24 h. Solution was dried at 79 °C following grinding, cooling, and calcination at 499 °C for 30 min [65]. Schematic illustration of these two methods is displayed in Fig. 4a.

The third method for TiO_2 nanoparticles was employed for the decomposition of polythene. TTIP (0.2 mL) was dissolved in ethanol (100 mL) and DI water (100 mL) following the addition of stabilizer tween 20 (4%) at different pH. The particles showed zeta potential at pH = 4 (50 °C). The obtained mixture was centrifuged (8000 rpm) and stirred (3 h) following the washing with DI water. Attained particles were employed for the degradation experiment [66].

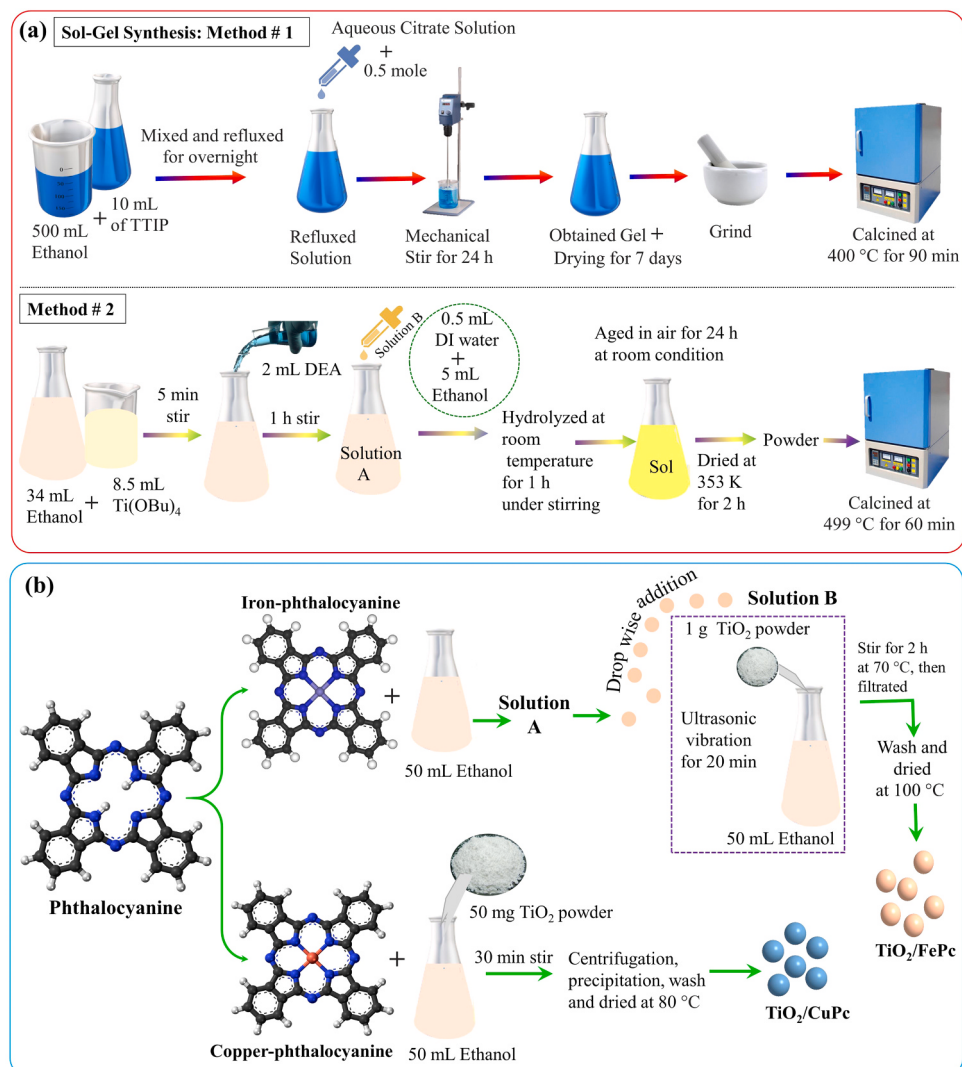


Fig. 4. (a) Sol-gel synthesis of TiO_2 by using two different methods. (b) Schematic illustration of FePc and CuPc modified TiO_2 .

4.2. Modified TiO_2

The photocatalytic performance of pure TiO_2 is limited due to the fast recombination of light-produced electron-hole pairs. Additionally, TiO_2 has a poor affinity for organics/pollutants treatment, especially in aquatic media. Numerous approaches have been developed to reduce the bandgap, electron-holes pairs recombination as well as improvement in degradation efficiency. Properties of modified TiO_2 are intrinsically different from pure TiO_2 with respect to charge separation, light absorption, contaminant adsorption, and ease of TiO_2 particle separation [40]. Modification of TiO_2 has been widely used to improve its performance and selectivity. Numerous reports are focused on TiO_2 modification especially for plastics degradation [67].

4.2.1. Phthalocyanine modified TiO_2

Phthalocyanine is a group of artificial pigments that comprises four isoindole components connected in a large ring. It has been considered an active material due to its chemistry and potential features such as electrical, optical, and magnetic [68–71]. For the preparation of FePc/ TiO_2 , 1 g commercial Degussa P25 (70% anatase and 30% rutile) powder was added in ethanol (50 mL) on ultrasonication for 20 min. FePc ethanol solution (50 mL) was added to TiO_2 solution in a dropwise manner and maintained on stir for 2 h at 70 °C following the filtration. Attained precipitates were washed many times with DI water and dried

at 100 °C. The obtained FePc/ TiO_2 was used for the degradation of polystyrene (PS) [72].

CuPc/ TiO_2 was prepared by two methods for the decomposition of PE and PS. In the first method, commercial TiO_2 (Degussa P25) was mixed in 50 mL ethanol-CuPc (2×10^{-5} M/L) solution following 30 min stir (for attaining the adsorption/desorption equilibrium). The solution was centrifuged, washed (many times with DI water), and dried (80 °C) [73]. In the second method, TiO_2 was synthesized by a sol-gel method employing the precursor solution of TiCl_4 . 0.2 g of prepared TiO_2 was mixed in ethanol (50 mL) following the stir for 30 min at 80 °C. Latterly, 100 mL ethanol-CuPc (2.4×10^{-5} M/L) solution was added to the TiO_2 solution. The mixture was centrifuged, and powder was washed with DI water and dried at 70 °C [74]. The modification method of TiO_2 with phthalocyanine is shown in Fig. 4b.

4.2.2. Vitamin C modified TiO_2

Vitamin C (0.1 g) was mixed in 10 mL tetrahydrofuran and DI water (named solution-A). 0.2 g of commercial TiO_2 (Degussa P25) was mixed in 30 mL tetrahydrofuran solution following the ultrasonication. 10 mL of solution-A was added dropwise in TiO_2 solution under magnetic stir leading to the formation of light-yellow suspension. This vitamin C modified TiO_2 was used for the degradation of polyvinylchloride (PVC) [75].

4.2.3. Protein-based nitrogen modified TiO_2

Extrapolial fluid from blue mussels (*Mytilus edulis*) was centrifuged (13,000 rpm) for 10 min. The fluid acts as a pore-forming agent and also a source of nitrogen. 5 mL extrapolial fluid into 1 mL of titanium butoxide was mixed for 2 h under stir (300 rpm). The solution was mineralized at room condition for 4 h subsequently transferred in Teflon lined autoclave at 150 °C with heating rate of 5 °C/min for 12 h. The powder was washed with DI water and dried at 55 °C [49].

4.2.4. Polyacrylamide modified TiO_2

Basically, there are two methods for the preparation of polyacrylamide modified TiO_2 . In the first method, the performance of TiO_2 was improved by adding the reactive double bond. Saline agent (3-trimethoxysilyl propyl methacrylate) was added in TiO_2 ethanol solution following the ultrasonication for 30 min and refluxed at 80 °C for 10 h. The resultant material was extracted with ethanol to remove the saline agent from TiO_2 nanoparticles. In the second method, MP_s- TiO_2 (20 g) was added in 200 mL DI water under 30 min sonication following stir for 20 min under a nitrogen atmosphere. The reaction temperature of the solution was increased up to 50 °C, then ammonium persulfate (0.34 g) and sodium hydrogen sulfite (0.16 g) was added. The grafting process starts with the addition of a monomer (21.32 g acrylamide in 100 mL aqueous solution) after 30 min of reaction, and the reaction proceeds at 50 °C for 3 h. The suspension was washed, filtrated, extracted and the catalyst was isolated under vacuum at 60 °C [76].

4.2.5. Mesoporous nitrogen modified TiO_2

Mesoporous nitrogen modified TiO_2 was synthesized by evaporation-induced self-assembly technique using the triblock copolymer (Pluronic F127 as a pore-forming agent) and urea (as nitrogen source). Triblock copolymer (9.1×10^{-6} M) was added in ethanol (0.728 M) following the dropwise addition of titanium chloride (0.0182 M) under 5 min stir. Finally, DI water (0.182 M) and urea (2.5×10^{-3} M) were mixed in the above solution under 5 min stir. The material was deposited on a glass substrate by using the dip coater, and the coating was exposed to water vapor for 30 s. The resultant coating was kept at 200 °C for 24 h to stabilize the material [77].

4.2.6. Polyoxometalate modified TiO_2

Phosphotungstic acid (3 mg) was dissolved in tetrahydrofuran (50 mL) following the addition of DI water. TiO_2 powder (100 mg) was added to the above solution, and dispersion was carried out by ultrasonication for 25 min. Laterly plastic was mixed in solution, and the prepared mixture was coated on a substrate with the help of spin coater [78].

4.2.7. Natural modified TiO_2

Synthetic rutile phase TiO_2 was extracted from leucoxene (a natural ore) which was named L. After its preparation through the ball-milling planetary method, it was mixed with commercial anatase at a ratio of 20: 80 following the mixing through milling machine at 400 rpm for 30 min [79].

4.2.8. DMC modified TiO_2

Dimethylcyclotrisiloxane (20 g) was added in ethanol (2 L) following the addition of TiO_2 (1 Kg) in the solution. The solution was allowed to evaporate in a rotary evaporator and dried at 100 °C for 2 h. Finally, the plastic was mixed with the resultant powder by melt blending technique, which was used for degradation reaction [80].

4.2.9. Bismuth oxyiodide modified TiO_2

Bismuth nitrate hexahydrate (4 mM) was added in ethylene glycol solution with a stoichiometric quantity of potassium iodide (4 mM) under 30 min stir following the transfer in an autoclave (sustained at 160 °C for 12 h). Obtained precipitates were washed with ethanol and DI water. BiOI (0.01 g) was added in ethanol (40 mL) under

ultrasonication for 30 min, TiO_2 was dispersed in the above solution under magnetic stir and infrared light irradiation until the evaporation of ethanol, and the obtained powder was dried at 100 °C for 24 h [81].

4.2.10. $Fe(St)_3$ modified TiO_2

Ferric stearate (0.003 g) and TiO_2 powder were added in tetrahydrofuran (5 mL), following the mixing with KH550 silicone on 20 min ultrasonication. This suspension was coated on PS to get the plastic-photocatalyst mixture under 12 h stir. Laterly the obtained material was transferred on a glass stick and dried for 48 h at room condition [82].

4.2.11. Graphene oxide reduced TiO_2

Graphene oxide reduced TiO_2 was prepared in three steps. In the first step, titanium butoxide (4 mL) was chelated in ethylene glycol (90 mL) under overnight stir condition (named solution-A) while the solution B was synthesized with 300 mL acetone addition in DI water (5 mL) following the addition of glacial acetic acid (molar ratio of glacial acetic acid: titanium butoxide = 3.5). In order to obtain the white precipitates, solution-A was added dropwise in solution B. Titanium glycolate precipitates were added in DI water (50 mL) to remove the remaining ethylene glycol under magnetic stir at 70 °C for 5 h. The obtained white powder was calcined at 500 °C for 3 h. In the second step, graphene oxide was prepared by the Hummers method. Thirdly, graphene oxide reduced TiO_2 was prepared by dispersing the graphene oxide in DI water (10 mL) and ethanol (5 mL) under ultrasonication following the addition of TiO_2 (0.1 g) nanoparticles, and the solution was stirred for 2 h. The resultant solution was transferred to autoclave and kept at 120 °C for 3 h. During the hydrothermal process, graphene oxide changes to reduced graphene and deposits on TiO_2 particles, as shown in Fig. 5 [83]. This prepared photocatalyst was employed for the degradation of PP under solar light irradiation but the weight loss percentage was not presented.

4.2.12. Amine modified aromatic polyamide dendrimer TiO_2

TiO_2 (0.5 M) was added in dichloromethane (50 mL) under ultrasonication for 60 min with subsequent dropwise addition of dicyclohexylcarbodiide (0.25 M), 4-dimethylamino pyridine (0.02 M), 5-diaminobenzoic acid (0.1 M), and methacryloxy propyl trimethoxyl silane in the above solution under nitrogen stir condition. Formed suspension was stirred at room condition for 10 h, centrifuge, and washed many times with dichloromethane. The obtained material was dried at 60 °C under a vacuum condition (named Solution 1). Solution 1 was added in 50 mL dichloromethane on sonication for 60 min, then dicyclohexylcarbodiide (0.75 M), 4-dimethylaminopyridine (0.06 M), 5-diaminobenzoic acid (0.6 M) were added drop by drop in the above solution under stirred condition. Formed suspension was kept at room condition for 16 h, centrifuged, washed, and dried at 60 °C under a vacuum condition (named as 2). Solution 2 was dispersed in ethanol (50 mL) under sonication for 60 min, then triacetoneamine (0.4 M) was added drop by drop in the above solution under nitrogen stir. The resultant ethyl alcohol was refluxed on 22 h stir and the resultant material was centrifuged, washed, and dried at 60 °C under vacuum condition named 3. Solution 3 was added in ethyl alcohol (50 mL) on sonication for 60 min following the stir for 2 h at 35 °C. Styrene (20 mL) was dissolved in 0.18 g of azobisisobutyronitrile and refluxed on nitrogen stir. The obtained mixture was centrifuged, extracted three times by toluene, vacuum dried at 100 °C, and the material was stored under dark condition [84].

4.2.13. Ascorbic acid modified TiO_2

The ascorbic acid modification was carried out through the incipient wet method. In one beaker, TiO_2 powder (3 g) was added to DI water (50 mL), while in another beaker ascorbic acid (1.5 g) was added to DI water (50 mL). The ascorbic acid solution was added to TiO_2 solution following 30 min stir. During this time, the solution starts changing its

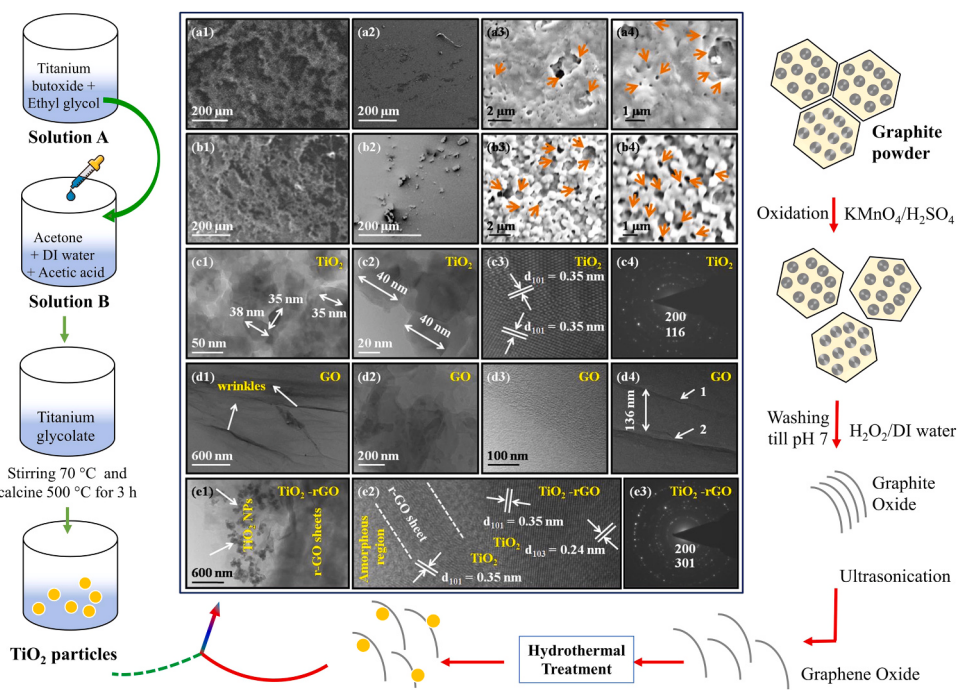


Fig. 5. Schematic illustration of graphene oxide reduced TiO_2 . Figure reproduced with permission from Ref. [83]. Copyright 2017 Elsevier.

color into beige yellow, indicating the occurrence of a chemical reaction. Precipitates were collected, washed, and heat-treated at 120 °C for 12 h [85].

4.2.14. Ethanol and surfactant modified TiO_2

Commercial TiO_2 powder was ground in a mortar, and the stuck material was removed through a spatula. After this 1 mL of DI water and Triton X-100 (300 μL) was added drop by drop to TiO_2 until it turns into a paste. Meanwhile, ethanol-modified TiO_2 was prepared by adding the 15 mL ethanol in fine ground TiO_2 powder. The obtained paste was ultrasonicated for 30 min following 40 min stir. Pastes were dropped on a substrate through the drop coating method. The substrate was dried at 70 °C calcined at 450 °C for 30 min [86].

4.2.15. Functionalized TiO_2

Functionalization is also considered an effective technique for improving the performance of TiO_2 . In this method, TiO_2 was dispersed in ethanol on sonication for 30 min (total 3 cycles and time for one cycle was 10 min with 5 min rest). The solution was stirred until it reaches 65 °C. At this stage, hexadecyltrimethoxysilane was added dropwise based on the desired concentration of functionalization; the temperature was increased to 78 °C and refluxed (3 h). The obtained material was washed and vacuum dried at 80 °C for 12 h [87].

4.3. Doped TiO_2

TiO_2 has been doped to increase its activity, and doping introduces extra energy in the band structure, which can play a role in the successful transfer of charges to the surface. Doping of TiO_2 has been mentioned below:

4.3.1. Transition Metal Loaded TiO_2

In order to decompose the plastics, transition metal silver (Ag) has been loaded on TiO_2 for improving its activity. The molar ratio of titanium n butoxide: ethanol (18): acetylacetone (0.5): DI water (2): nitric acid (0.2). These chemicals were mixed under stir at room temperature for 1 h. Meanwhile, silver nitrate was synthesized by adding the AgNO_3

to ethanol. After this, prepared silver nitrate solution was added in TiO_2 , stirred, and refluxed at 80 °C for 8 h [88].

4.3.2. Carbon-nitrogen TiO_2

Extrapolial fluid (as doping source) was used to enhance the performance of TiO_2 . Extrapolial fluid (*Mytilus edulis*) was removed with a syringe and centrifuged (13,000 rpm). Resultant extrapolial fluid (20 mL) was added in titanium butoxide (0.01425 M) under 2 h stir. After 4 h mineralization, the mixture was poured into a Teflon-lined autoclave and kept at 150 °C for 12 h. The resultant product was washed with DI water and dried at 55 °C for 12 h [89].

4.3.3. Graphite doped TiO_2

Actually, the graphite-doped TiO_2 was prepared with a plastic sample. PVC (2 g), N, N dimethylformamide (15 g), TiO_2 (1 wt%), and graphite (1 wt%) were mixed under stir at 60 °C for 1 h following the ultrasonication for 10 min. The resultant material was evenly spread on a substrate through a scraping machine, and the film thickness was 150 μm . The film producing plate was removed and immersed in DI water to produce graphite doped TiO_2 -PVC film [90] as shown in Fig. 6.

4.4. Nano TiO_2

The fabrication of nano TiO_2 consists of two parts. TiO_2 nanoparticle grafting was done by adding and dissolving 5 mL of WD-70 (silicon coupling agent) in isopropanol (125 mL) following the addition of TiO_2 powder (50 g) under sonication for 20 min. The suspension was transferred to a Wolff bottle, stirred at 35 °C for 2 h. Styrene monomer (25 mL) was dissolved in azobisisobutyronitrile (0.2 g), and the solution was refluxed on stir at 80 °C for 20 h under nitrogen condition. Latterly, the resultant material was centrifuged, and the prepared catalyst was washed three times with toluene and dried under vacuum conditions at 110 °C. Secondly, the composite film was prepared by adding the graphite doped TiO_2 (0.15–0.16 g) in trichloromethane (100 mL) through sonication for 20 min following the addition of styrene particles (30 g) on a continuous stir for 5 h. The mixture was spread over the ceramic plate and dried for 48 h [91].

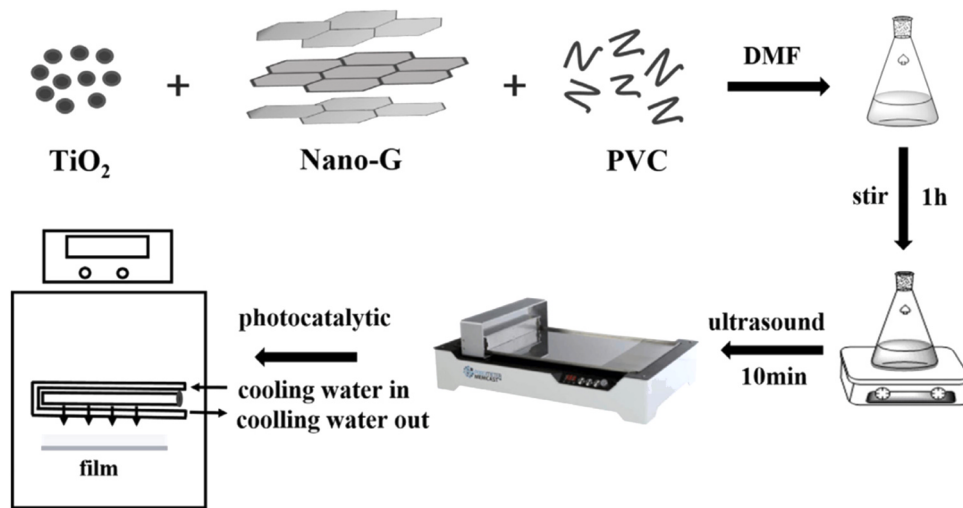


Fig. 6. Flow chart illustration of graphite doped TiO_2 -PVC film.
Figure reprinted with permission from Ref. [90]. Copyright 2020 Elsevier.

4.4.1. Multi-walled carbon nanotube TiO_2

Multi-walled carbon nanotube TiO_2 was prepared in two steps (Fig. 7). In the first step, a multi-walled carbon nanotube was purchased and treated with the acid vapor technique. In order to remove the amorphous carbon, a multi-walled carbon nanotube was calcined at 450 °C for 1 h. A multi-walled carbon nanotube was loaded on a silicon griddle in a Teflon (nitric acid was already present in the bottom) following the heat treatment at 120 °C for 3 h. The obtained material was washed with DI water until it reaches pH = 7, then dried at 100 °C for 5 h. Secondly, titanium butoxide (4.4 mL) was added in ethanol (20 mL) under 10 min stir, named as A. Treated multi-walled carbon (50 mg) was dispersed in ethanol (20 mL) on sonication for 10 min following the addition of acetic acid (2 mL), while pH = 2–3 was regulated by nitric acid, named as B. A mixture was added gradually in B, then stirred for about 15 min. This solution was left for 1 h stir in a water bath at 60 °C, transferred in an autoclave, and heated at 180 °C for 6 h. During heat treatment, TiO_2 particles grow over the carbon nanotube generating the gray precipitates. The obtained product was washed with ethanol and dried at 90 °C for 6 h [92].

4.4.2. Perchlorinated iron phthalocyanine modified nano TiO_2

TiO_2 powder (1 g) was added to ethanol (50 mL) and sonicated for 20 min. FePcCl_{16} -ethanol (50 mL) was added dropwise in the above solution, and the quantity of FePcCl_{16} was 2% in TiO_2 . The suspension was stirred at 70 °C and cooled at room condition. The resultant material was washed and dried [93].

4.5. Poly (ethylene oxide) microcapsule TiO_2

Poly(ethylene oxide) and TiO_2 commercial products were used to synthesize poly(ethylene oxide) microcapsule TiO_2 by melting mixture. The material was mixed with and without the tetra N-methylated hindered amine (ADK STAB LA-52) and phenolic antioxidant (ADK STAB AO-60) on 60 rpm stir at 180 °C for 5 min [94].

5. Application for microplastics (MPs) degradation

The efficient performance of TiO_2 has been observed toward MPs degradation. Fig. 8a1–a6 presents the diameter change, degradation efficiency, and reaction end products on different films of TiO_2 for PS degradation. Fig. 8a1 displays a significant diameter change in 400 nm PS spheres, and a little change was observed on FTO. Triton X-100 (TXT) and ethanol (ET) based TiO_2 present a significant diameter change which was about 100.07 and 177.78 nm, respectively. While the water (WT) based TiO_2 showed 268.16 nm after 12 h reaction under 365 nm UV light irradiation. Efficient performance can be attributed to its band energy, particle size, surface area, charge separation, and light absorption. The degradation efficiency of 400 nm PS after 12 h reaction on TXT, ET, and WT was 98.40%, 91.04%, and 69.25%, respectively (Fig. 8a2). Fig. 8a3 shows the diameter change in 700 nm, 1 μm , and 5 μm PS. Diameter changes of 700 nm and 1 μm PS were about 251.96 nm and 401.28 nm, while their degradation efficacy was 95.30% and 93.49% after 24 h respectively under 365 nm UV light irradiation (Fig. 8a4). Efficient diameter changes in 5 μm PS were seen on TXT film under 254 nm UV light, and its degradation efficiency was 99.99% after

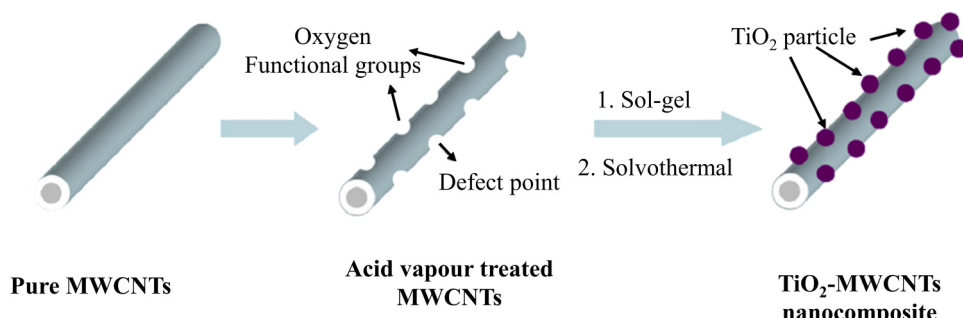


Fig. 7. Flow chart presentation of multi-walled carbon nanotube TiO_2 .
Figure reprinted with permission from Ref. [92]. Copyright 2014 Elsevier.

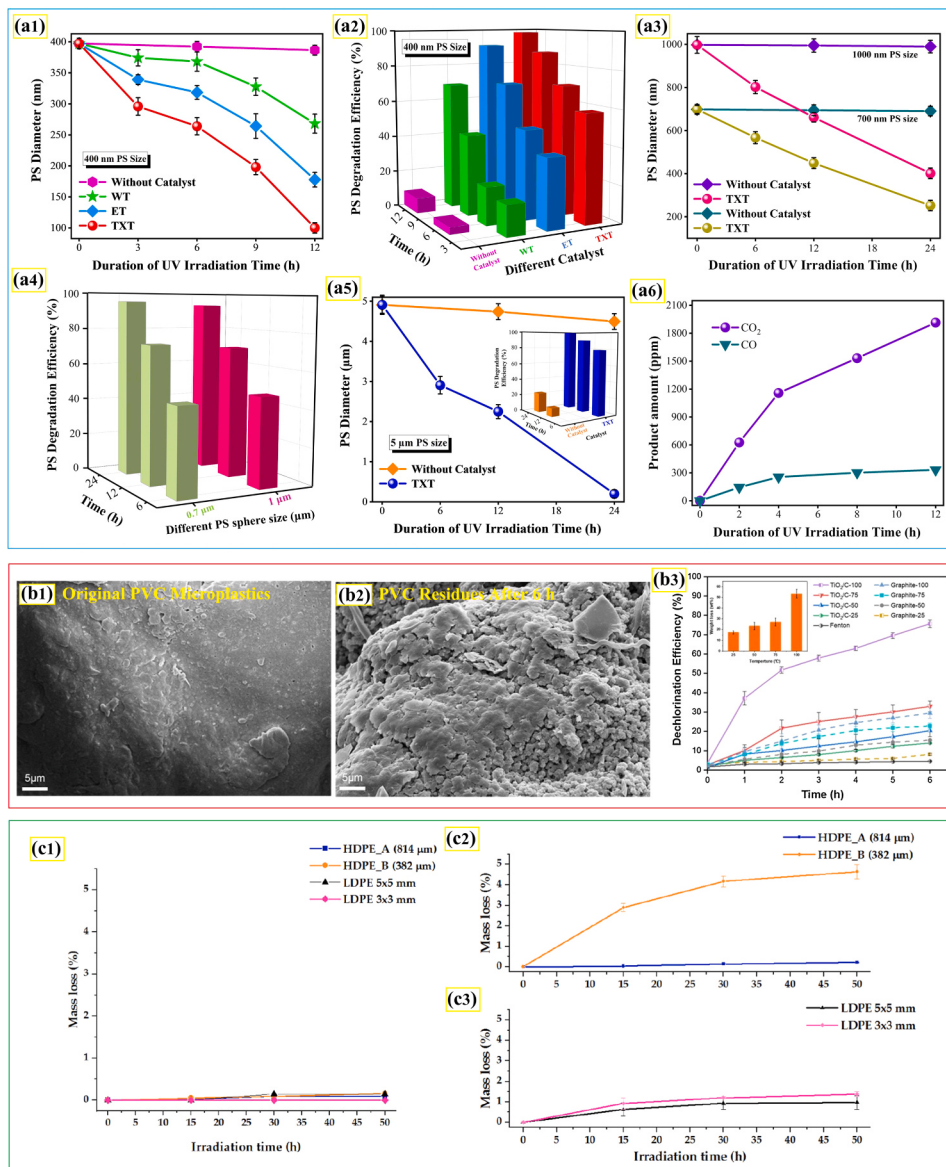


Fig. 8. (a1-a2) Diameter change (DC) and degradation efficiency (DE) of 400 nm PS on different fabricated TiO₂ films under 365 nm UV light. (a3-a4) DC and DE of 700 and 1000 nm PS on TXT film under 365 nm UV light (a5) DC and DE of 5 μm PS on TXT film under 254 nm UV light. (a6) Reaction product during the degradation reaction with TiO₂. (b1) Scanning electron microscopy (SEM) images of original PVC before reaction. (b2) SEM images of PVC sample after 6 h of electrocatalytic reaction. (b3) Dichlorination efficiency of PVC with TiO₂/C, and graphite at different temperatures and Fenton at 25 °C. (c1) Photolysis mass loss of HDPE and LDPE at pH = 3 under visible light irradiation. (c2) Mass loss of HDPE with N-TiO₂ at solution pH = 3 under visible light irradiation. (c3) Mass loss of LDPE with N-TiO₂ at solution pH = 3 under visible light irradiation.

(a6) Figure a1-a6 reproduced with permission from Ref. [86]. Copyright 2020 Elsevier.

(b3) Figure b1-b3 reproduced with permission from Ref. [95]. Copyright 2020 Elsevier.

(c3) Figure c1-c3 adopted from Ref. [77]. Copyright 2020 MDPI.

24 h reaction, while insignificant degradation was seen on FTO, as illustrated in Fig. 8a5. Furthermore, the reaction product during the degradation was also determined through gas chromatography. It can be seen in Fig. 8a6, the production of CO₂ increases linearly in the early stages and then decreases in the following steps. The production of CO₂ was much higher as compared to CO, which indicates mineralization [86].

PVC microplastic decomposition was carried out by electrolysis at -0.7 V vs. Ag/AgCl via TiO₂/C cathode [95]. The actual morphology of PVC before and after the electrocatalytic reaction is depicted in Fig. 8b1-b2. Notably, the PVC has a smooth surface before the reaction (Fig. 8b1), but a significant change such as holes and depression was seen after the reaction (Fig. 8b2). Mainly, the internal inside of PVC is exposed to degradation when the surface material is decomposed. The dichlorination efficacy of the system for PVC decomposition was determined under different temperatures, and the highest dichlorination efficiency and weight loss were 75% and 56% at 100 °C, respectively. Notably, the highest dichlorination efficacy was observed at high temperatures. Graphite cathode showed 29% dichlorination efficiency after 6 h reaction at 100 °C as displayed in Fig. 8b3. Dichlorination efficacy was also investigated by the traditional Fenton method at 25 °C, while

the efficiency was very low.

Fig. 8c1 illustrates the photolysis mass loss of HDPE and LDPE at pH = 3 under visible light irradiation. No efficient mass loss was observed without photocatalyst throughout the irradiation reaction which indicates that chromophore did not participate in degradation.

Fig. 8c2 shows the mass loss of HDPE MPs derived from commercial face products. HDPE-A shows a very limited mass loss after 50 h light irradiation with a mean value of 0.22%. This limited mass loss can be ascribed to intrinsic properties of MPs and huge size in comparison to catalysts. Additionally, the particle size of HDPE-B was also larger than the particle size of the catalyst. The total mass loss was 4.65% (orange line) seen with catalyst after 50 h of reaction. Moreover, the mass loss was also investigated for different sizes of LDPE. About 0.97% mass was observed for LDPE with size 5 × 5, while this value was 1.38% for LDPE 3 × 3 after 50 h of reaction with catalyst under visible light irradiation. This change in the mass loss was observed due to the reaction of reactive radical species [77]. Generally, the particle size and shape affect the degradation rate and the catalyst performance.

The photocatalytic degradation of HDPE was investigated through N-modified TiO₂ under different experimental conditions. The photodecomposition of HDPE is linked with the porosity of the catalytic

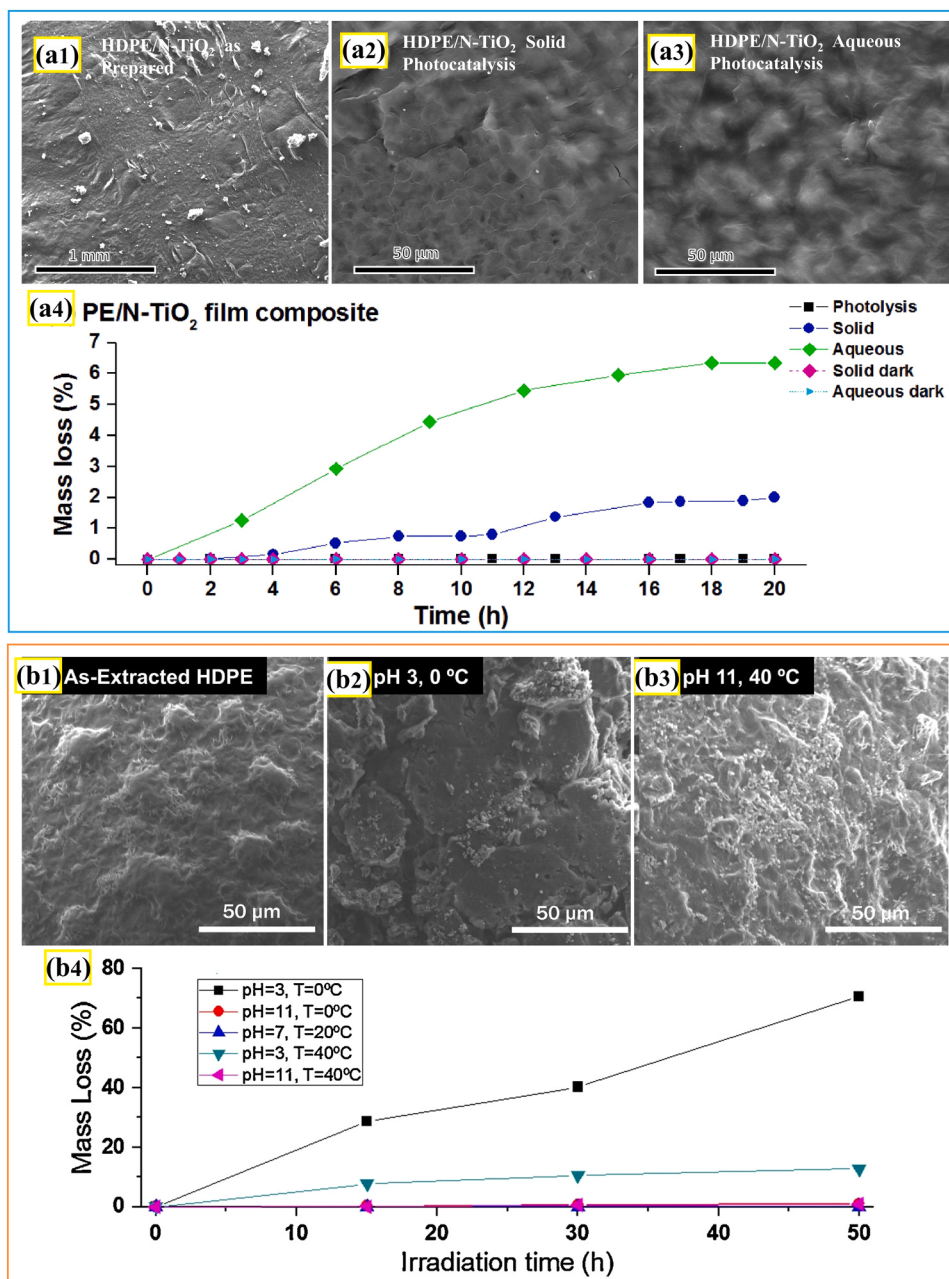


Fig. 9. (a1) SEM image of HDPE/N-TiO₂ as prepared composite. (a2) SEM image of HDPE/N-TiO₂ after solid-phase degradation. (a3) SEM image of HDPE/N-TiO₂ after aqueous phase degradation. (a4) Mass loss % vs. time for HDPE. (b1) SEM image of as extracted HDPE/C, N-TiO₂ as extracted. (b2) SEM image of as extracted HDPE/C, N-TiO₂ after degradation reaction at pH = 3 and 0 °C. (b3) SEM image of as extracted HDPE/C, N-TiO₂ after degradation reaction at pH = 11 and 40 °C. (b4) Mass loss of HDPE vs. time. (b4) Figure a1-a4 and b1-b4 reprinted with permission from Refs. [49] and [89]. Copyright 2019 and 2020 Elsevier, respectively.

material. Fig. 9a1–a3 shows the SEM images of catalyst-loaded HDPE before and after the degradation reaction. The actual morphology of HDPE with a catalyst (as prepared sample) shows the rough surface of the composite (Fig. 9a1). The high surface area of catalysts can enhance the interaction with plastic. Fig. 9a2 shows that HDPE/N-TiO₂ has a rough surface with porosity after solid-phase photocatalysis, while Fig. 9a3 displays a significant change in HDPE morphology after aqueous phase photocatalysis. A significant change in HDPE is associated with hydroxyl radical's production in an aqueous solution derived from the catalyst. These findings suggest that catalysts can degrade the MPs in the solid and aqueous phases. The mass loss % of HDPE vs. time under different conditions is presented in Fig. 9a4. The photolysis experiment showed limited degradation under visible light. About 6.40% mass loss of HDPE was observed with N-TiO₂ after 20 h reaction under visible light at room condition. The kinetic rate constant of the aqueous system was 3 times faster than the solid system [49]. Fig. 9b1 shows the extracted HDPE sample which indicates the non-porous

surface. The decomposition experiment disclosed that HDPE has cracks and cavities with a smooth surface (Fig. 9b2). These morphological changes are linked to the decomposition through the increased interface between HDPE MPs and C, N-TiO₂. The change in surface indicates decomposition and makes the inside material available for further disintegration [15].

Fig. 9b3 displays fewer degradation at pH = 11 and 40 °C with C, N-TiO₂. The overall mass loss at different pH and temperature is shown in Fig. 9b4. The highest mean weight loss was 71.77% at pH = 3, temperature 0 °C after 50 h reaction under visible light irradiation. These findings suggest that pH and temperature play a role in MPs decomposition. Meanwhile, the mean mass loss was 12.42% at pH = 3, temperature 40 °C after 50 h reaction, which was one-sixth of attained at pH = 3 (0 °C). About 0.47% of mass loss was seen at pH = 7 (20 °C). The mass loss at basic pH = 11 was 1.55%, 0.78% at 0 °C, and 40 °C, respectively. Temperature and solution pH affect degradation and mean weight loss [89]. All fabricated TiO₂ films showed efficient performance

toward the MPs degradation under different experimental conditions.

6. Application for macro plastic degradation

Pure and modified TiO₂ has been used for the decomposition of macro plastic debris, which is the most noticeable pollution at beaches and shores. Fig. 10a1–a6 displays the morphological change of TiO₂-PVC film before and after light irradiation. Fig. 10a1 and a4 shows the smooth surface morphology of PVC film with pure and vitamin C modified TiO₂ before irradiation. A significant change in PVC film morphology was observed upon light irradiation, indicating the decomposition with pure (Fig. 10a2-a3) and vitamin C modified TiO₂ (Fig. 10a5-a6). Cavity formation signifies the photodegradation reaction initiation at the interface of PVC and catalyst. Interestingly, the cavity

size and depth of vitamin C modified TiO₂ loaded PVC film was much bigger as compared to pure TiO₂ loaded PVC film [75].

The degradation of PE was carried by using transition metal modified TiO₂. Fig. 10b1 shows that PE has a smooth surface before the irradiation reaction, while a change in PE morphology (holes and cavities) was observed after 300 h degradation reaction under UV light (Fig. 10b2). The morphology of PE with pure, Fe, Ag, and Fe/Ag-doped TiO₂ under UV light are shown in Fig. 10b3–b6. The efficient change in morphology was noticed through Ag and Fe/Ag-doped TiO₂. Cavity formation was observed due to the attack of active oxygen radical species and the escape of volatile products [96]. Bismuth oxy-iodide-modified TiO₂ was also employed for improving the activity of pure TiO₂. Fig. 10c1 and c2 show the morphology of PVC-TiO₂ and PVC-BiOI/TiO₂ before the degradation. Surface changes in PVC-BiOI/TiO₂ after 72 h (Fig. 10c4)

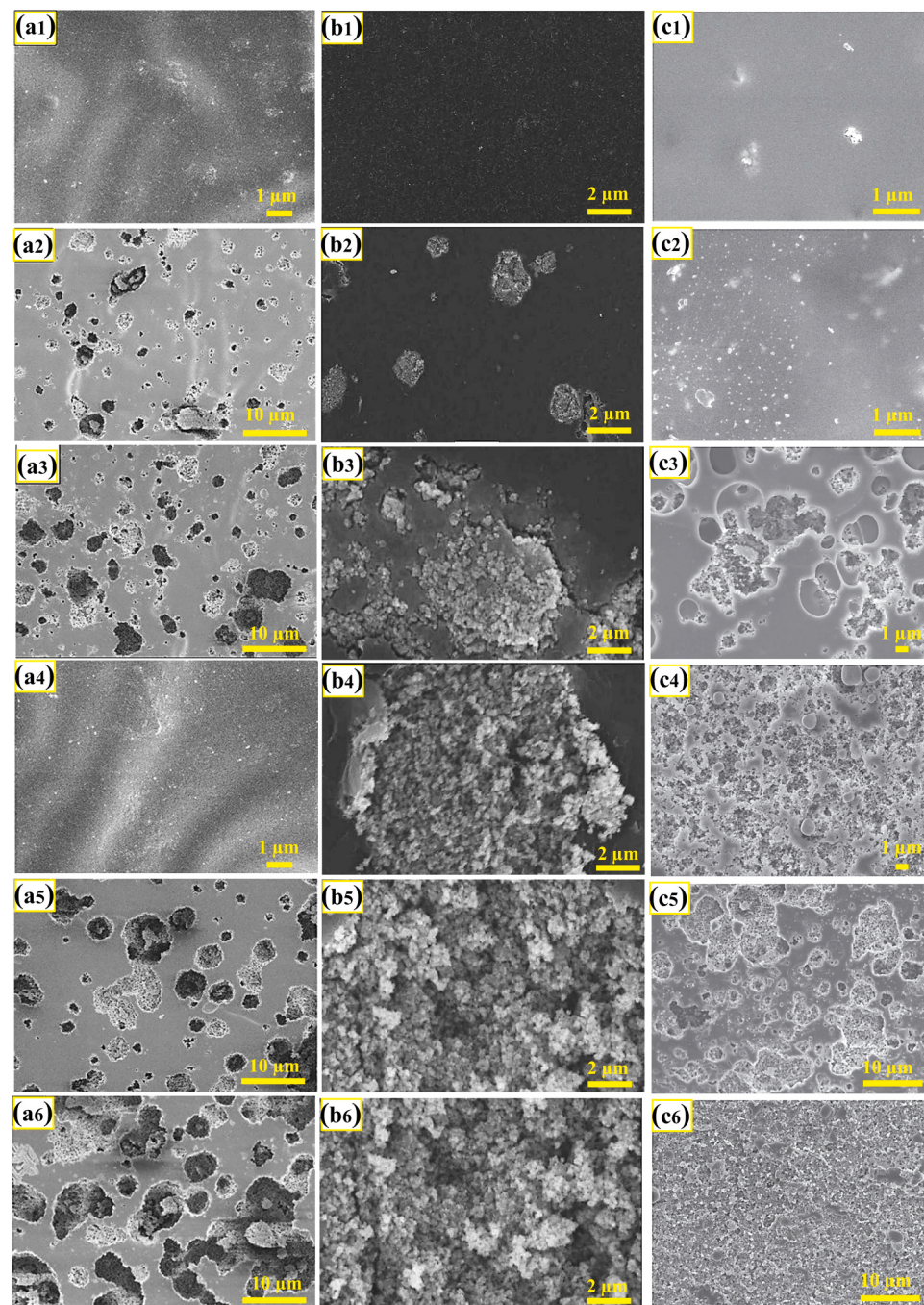


Fig. 10. (a1) SEM image of PVC-TiO₂ before reaction. (a2) PVC-TiO₂ after 70 h reaction. (a3) PVC-TiO₂ after 100 h reaction. (a4) PVC vitamin C modified TiO₂ before reaction. (a5) PVC vitamin C modified TiO₂ after 70 h reaction. (a6) PVC vitamin C modified TiO₂ after 100 h. (b1) SEM image of PE before reaction. (b2) PE-TiO₂ after reaction. (b3) PE-TiO₂ after reaction. (b4) PE-Fe doped TiO₂ after reaction. (b5) PE-Ag doped TiO₂ after reaction. (b6) PE-Fe/Ag doped TiO₂ after reaction. (c1) SEM image of PVC-TiO₂ before reaction. (c2) PVC-BiOI/TiO₂ before reaction. (c3) PVC-TiO₂ after 72 h reaction. (c4) PVC-BiOI/TiO₂ after 72 h reaction. (c5) PVC-TiO₂ after 169 h reaction. (c6) PVC-BiOI/TiO₂ after 169 h reaction.

(a6) Figure a1–a6 reproduced with permission from Ref. [75]. Copyright 2010 Elsevier.
(b6) Figure b1–b6 reprinted from Ref. [96]. Copyright 2011 Hindawi.
(c6) Figure c1–c6 reproduced from Ref. [81]. Copyright 2011 Wiley.

and 169 h (Fig. 10c6) were more effective than PVC-TiO₂ after UV light irradiation (Fig. 10c3 and c5) [81].

Perchlorinated iron phthalocyanine is proven as a stable catalyst even for 4 weeks than FePc for the oxidation of cyclohexane, suggesting the significant performance of phthalocyanine toward pollutant degradation [97]. Fig. 11a1 displays the smooth surface morphology of PVC loaded with FePcCl₁₆-TiO₂ at 0 h. Few changes in PVC film were seen without photocatalyst after 240 h UV reaction (Fig. 11a2). PVC-loaded TiO₂ film showed broken segments and cavities, as illustrated in Fig. 11a3. Nevertheless, the PVC-loaded FePcCl₁₆-TiO₂ showed a huge number of broken fragments and dense cavities under the same reaction condition (Fig. 11a4). Fig. 11a5 presents the weight loss of PVC with and without photocatalyst under sunlight (intensity 4.2 mW/cm²) carried out in Wuhan city, China. The highest weight loss of PVC was observed with FePcCl₁₆-TiO₂ than pure TiO₂. Additionally, the photolysis of PVC showed negligible weight loss [93].

Different concentrations of copper phthalocyanine (CuPc) were loaded on TiO₂ for the degradation of PE under sunlight. The weight loss of pure PE was negligible after 160 h irradiation. Loading of TiO₂ with PE leads to little weight loss, but the coupling of TiO₂ with copper phthalocyanine showed remarkable performance (Fig. 11b1). The apparent decomposition rate was 0.7% with CuPc/TiO₂, which corresponded to 0.3 monolayers of CuPc on TiO₂ (Fig. 11b2). These findings imply that a combination of CuPc and TiO₂ can introduce more active species generation for PE degradation, bond cleavage, and volatile product formation [73]. Meanwhile, the performance of CuPc/TiO₂ was also tested for the decomposition of PS (Fig. 11b2). The weight loss % of PS was much higher with CuPc/TiO₂ as compared to pure TiO₂. About 6.9% weight loss of PS was observed with CuPc/TiO₂, while this weight loss was 4.1% after 250 h. The weight loss % was faster in the initial stage and slower in the subsequent phase. Chain scission in polymers takes place randomly, and a rapid initial weight loss slows the continuous process [74].

Fig. 11d1-d2 illustrates the weight loss of PS with FePc modified TiO₂ under different UV light intensities. The highest weight loss of PS was observed with FePc-TiO₂ (1 wt% TiO₂) through different films and the degradation rate increase with an increase in reaction time. Total 65%

and 82% reduction of PS was observed after 480 h with light intensity 1 and 2 mW/cm². However, pure TiO₂ showed 21% and 25% decomposition after 480 h under the same reaction condition. The weight loss of FePc-TiO₂ at low UV light intensity was efficient in comparison with pure TiO₂ [72].

Fig. 12a displays the physical shape of PE film before and after solar light irradiation. It can be seen that the brittleness of film and pores formation was increased after reaction which indicates the efficient degradation. Notably, 0.1 wt% of TiO₂ loaded in LDPE showed efficient decomposition in an eco-friendly way [98]. The nature of thin PVC film and PVC blended TiO₂ film is shown in Fig. 12b1-b2. PVC film has a smooth, and transparent surface. TiO₂ particles were embedded in PVC film, and the transparent structure helps UV light absorbance, which enhances the degradation rate. Fig. 12b3 shows that TiO₂ blended PVC film exhibits a huge number of fragments after 20 days of UV light (Fig. 12b3) [99].

The PS film incorporated TiO₂ film showed higher weight loss than PS film only (Fig. 12c). About 29% weight loss of PS was observed with 1 wt% grafted TiO₂, while PS-loaded TiO₂ showed 13% under UV light [91]. TiO₂(P25) presented 18% weight loss while multiwalled carbon nanotube with carbon concentration 5%, 10%, 20% and 40% loaded TiO₂ showed 28%, 29%, 35% and 24% after 180 h irradiation (Fig. 12d) [92]. Fig. 12e shows the weight loss of PVC film with pure and nano graphite modified TiO₂. The highest weight loss of PVC film was observed by nano graphite doped TiO₂. The weight loss of PVC with nano graphite, pure TiO₂, and nano graphite modified TiO₂ was 7.68%, 8.94%, and 17.24%, after 30 h, respectively. Nano graphite exhibits a multi-layered sheet-like monoclinic shape, which allows the easy blending of TiO₂ and well dispersion of PVC resulting in improved performance of catalyst [90].

Fe(St)₃ modified TiO₂ has been used for the degradation of PS film under UV light. The highest weight loss (22%) was observed with Fe(St)₃ modified TiO₂ after 288 h (Fig. 12f). Photodegradation of PS film showed only 10% weight loss, while a 15% reduction in PS was observed with pure TiO₂. The addition of Fe(St)₃ can improve the photocatalytic performance for plastic degradation with uniform dispersion [82]. Functionalization improves the distribution of polymer and catalyst. The

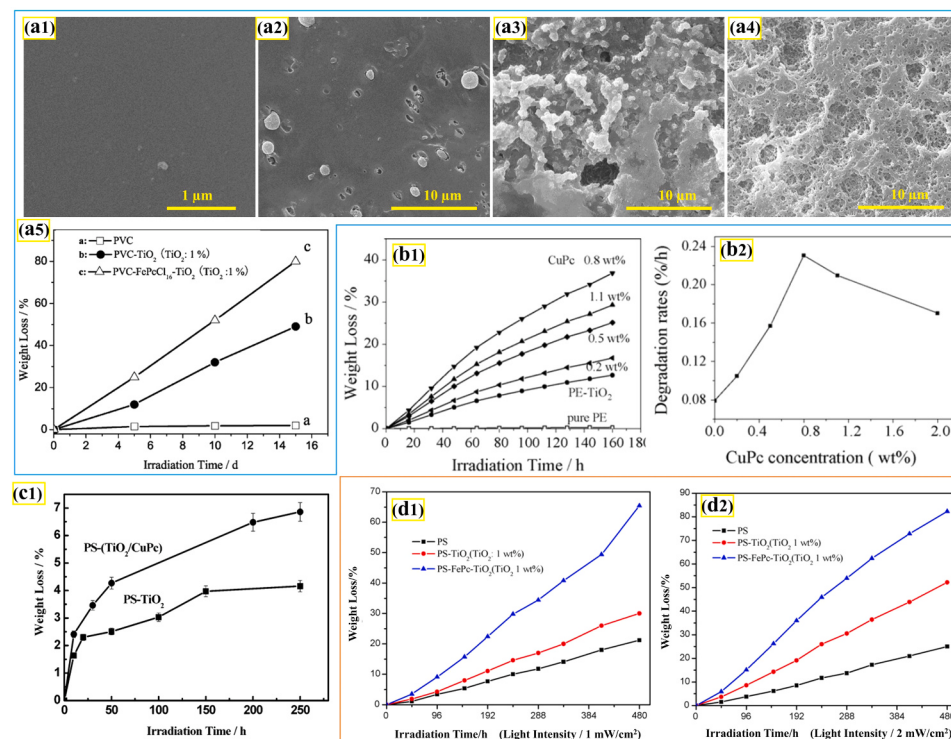


Fig. 11. (a1) SEM image of PVC loaded with FePcCl₁₆-TiO₂ at 0 h of reaction. (a2) PVC film without catalyst after 240 h reaction. (a3) PVC-TiO₂ after 240 h reaction. (a4) PVC loaded with FePcCl₁₆-TiO₂ after 240 h. (a5) PVC weight loss vs. irradiation time. (b1) PE weight loss vs. irradiation time with and without photocatalyst. (b2) PE degradation rates % vs CuPc concentration. (c) PS weight loss % vs. irradiation time with pure and modified TiO₂. (d1) Weight loss of PS with and without catalyst under UV light intensity 1 mW/cm². (d2) Weight loss of PS with and without catalyst under UV light intensity 2 mW/cm². (a5) Figure a1-a5 reproduced from Ref. [93]. Copyright 2011 Wiley. (b1-b2) Figure b1-b2 reproduced with permission from Ref. [73]. Copyright 2008 Elsevier. (c) Reproduced with permission from Ref. [74]. Copyright 2003 American Chemical Society. (d1-d2) Figure d1-d2 reprinted with permission from Ref. [72]. Copyright 2008 Elsevier.

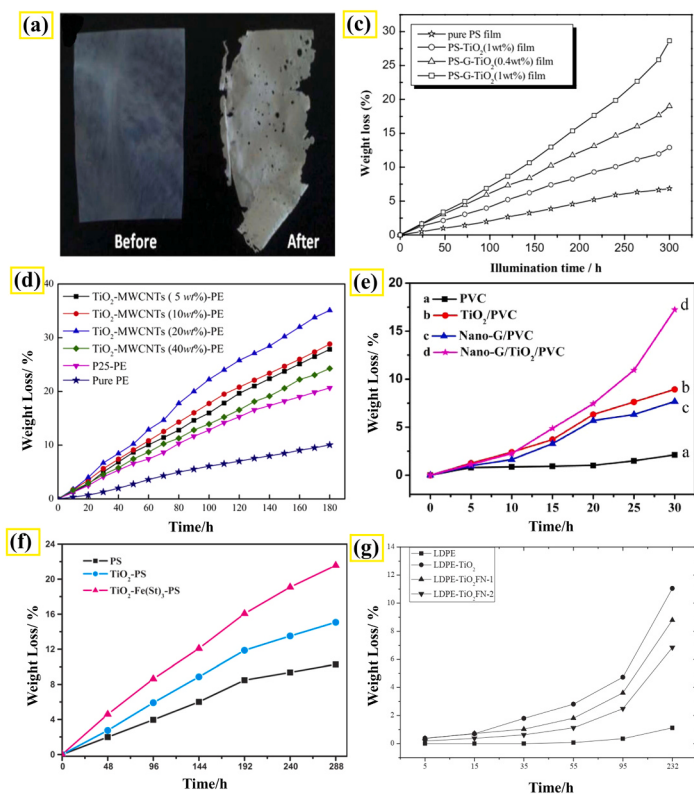


Fig. 12. (a) Photograph of PE before and after the reaction under solar light. (b1) Photograph of PVC thin film. (b2) The PVC-TiO₂ film before reaction. (b3) PVC-TiO₂ film after 20 days reaction under UV light. (c) PS weight loss % vs. irradiation time with pure and modified TiO₂. (d) Weight loss of PE with different concentrations of multi-walled carbon nanotube and without a catalyst. (e) Weight loss of PVC with and without a catalyst. (f) Weight loss of PS with ferric stearate modified TiO₂ and without a catalyst. (g) Weight loss of LDPE with functionalized TiO₂ and without a catalyst.

(a) Figure reproduced from Ref. [98]. Copyright 2013 Royal Society of Chemistry. (b3) Figure b1-b3 reproduced with permission from Ref. [99]. Copyright 1998 American Chemical Society. (c) Figure reproduced with permission from Ref. [91]. Copyright 2004 Elsevier. (d) Figure reprinted with permission from Ref. [92]. Copyright 2014 Elsevier. (e) Figure reproduced with permission from Ref. [90]. Copyright 2020 Elsevier. (f) The figure is adopted from Ref. [82]. Copyright 2012 Wiley. (g) Figure reproduced with permission from Ref. [87]. Copyright 2016 Elsevier.

unfunctionalized TiO₂ showed 11% PVC weight loss while this value was 7% and 9% with functionalized TiO₂ (Fig. 12g) [87]. The overall macro and micro-plastics degradation efficiency with remarks and limitations is presented in Table 1.

7. Conclusions and future recommendations

Plastics are a persistent man-made pollutant that has become a global problem due to their ubiquitous presence and unknown threat to living organisms. It is anticipated that macro and micro-plastic contamination will cause serious harm to various ecosystems due to the increasing worldwide manufacturing and use of plastics. The photocatalytic technique has been successfully used in recent years and significant advancement has been made towards the sustainable decompositions of macro and micro-plastics. Since polymers could be self-decomposable to some extent, ensuing in the break down into small plastics wrecks. Finding the decomposition techniques to eliminate the macro and micro-plastics effectively is gaining growing attention. TiO₂ based photocatalysis has been typically highlighted as a potential method for plastics treatment. This review covers the recent progress of macro and micro-plastics degradation through TiO₂ photocatalyst. Additionally, the preparation methods of TiO₂ for macro and micro-plastics degradation have been enumerated. The physicochemical features such as catalytic performance, and stability of TiO₂ that make it a suitable candidate for plastics degradation have been investigated. Since the TiO₂ photocatalytic technique cannot accomplish complete plastics mineralization under visible light, the improvement in TiO₂ photocatalyst may be a future developmental trend, resulting in enhanced degradation efficiency. A degradation mechanism of TiO₂ employed for plastics has been proposed. Light-induced active species such as holes, •OH, and O₂[•] play a vital role in macro and micro-plastic decomposition. The degradation pathway of macro and micro-plastics usually refers to the bond cleavage of polymer chains due to the action of active species. Furthermore, temperature and solution pH have shown a remarkable effect on micro-plastics degradation but till now, these factors have not

been studied for macro-plastics degradation. Most of the modified TiO₂ does not show the complete degradation of macro and micro-plastics, and the degradation efficiency of TiO₂ requires further improvement. The coupling of carbon, nitrogen, vitamin C, and FePcCl₁₆ with TiO₂ enhanced its performance to some extent for specific plastics decomposition.

Although many efforts have been made for macro and micro-plastics degradation, it should be acknowledged that there are still knowledge gaps to be studied such as optimization of TiO₂ in terms of its degradation performance, reusability, cost, and environmental friendliness. To date, TiO₂ based photocatalysts, which are chiefly bound in the UV region, have been distinctively highlighted as the potential material. Hence, there is a need to develop novel and efficient visible-light-driven TiO₂ based photocatalytic material. Additionally, most of the current studies are focused on specific types of macro and micro-plastics degradation while TiO₂ based photocatalytic system should efficiently decompose from single to multiple types of polymers. More investigation of TiO₂ photocatalytic decomposition of nano plastics and reaction intermediates toxicity is required. Since the photodecomposition of macro and micro-plastics are complex, it is crucial to expound and figure out the role of major reactive radical species for different types of plastic decomposition. There is a need to evaluate the degradation performance of TiO₂ for real water enriched MPs solution. The photoreaction chamber which constitutes numerous vital engineering variables has gained remarkable attention. An innovative method for macro and micro-plastics removal, particularly for simultaneous collecting and removing from aquatic media, is a floating photoreaction chamber with TiO₂ material. This photo chamber, which is towed by a boat sailing on the water, could efficiently remove the floating plastic particle in the sea or ocean under natural sunlight. To promote this method, future studies should pay special attention to tailoring novel catalytic materials.

Declaration of Competing Interest

The authors declare that they have no known competing financial

Table 1Application of TiO₂ for the degradation of plastics.

Catalyst	Target Plastic	Degradation Efficiency	Light Source	Remark	Limitation	Reference
Triton X-100 based TiO ₂	400 nm PS	98.40% after 12 h	365 nm UV light	The performance of TiO ₂ was significantly improved with ethanol and surfactant.	Only work under UV light irradiation.	[86]
	MPs PE	Complete decomposition after 36 h	254 nm UV light	Degradation was more effective in the solid phase.		
Ethanol based TiO ₂	400 nm PS	91.04% after 12 h	365 nm UV light			
N-TiO ₂ (Prepared from extrapallial fluid)	MPs HDPE (diameter 700–1000 μm)	6.40% after 20 h	Visible light	Extrapallial fluid extracted from fresh blue mussel showed efficient performance as compared to sol-gel synthesized TiO ₂ .	Decomposition performance is negligible, and photocatalysis of HDPE microbeads needs further investigation.	[49]
C, N-TiO ₂	MPs HDPE	71.77 ± 1.88% after 50 h	Visible light	HDPE degradation was affected by solution pH and temperature.	Require further improvement and need testing for other plastics.	[89]
TiO ₂ /graphite cathode	MPs PVC	56% at 100	–	Remarkable efficiency for PVC decomposition through cathodic reduction and OH oxidation.	It is a temperature-dependent approach that is not suitable for real application.	[95]
Mesoporous N-TiO ₂	MPs HDPE MPs LDPE	4.65% after 50 h 1.38%	Visible light	Smaller-sized MPs lead to higher decomposition, while film MPs showed lower degradation.	Mass loss is insignificant.	[77]
TiO ₂ multi-walled carbon nanotube	PE film	35% after 180 h	UV light	The acid vapor method synthesized multi-walled carbon nanotube modified with sol-gel synthesized TiO ₂ is an inspiring approach for plastic degradation under a mercury lamp.	There is a need to explore the reaction intermediates.	[92]
TiO ₂ /Fe(St) ₃	PS	Average molecular weight decreased to 79.49% after 480 h	UV light	Ferric stearate improves the PS dispersion and catalyst performance.	It is a UV light-dependent system and produces products that need biodegradation. Mass loss is not present, which is a limitation in this study.	[82]
TiO ₂	PVC film	–	UV light	Thin-film of PVC decomposed faster than PVC particles by TiO ₂ .		
Functionalized TiO ₂	LDPE	–	UV light	Hexadecyltrimethoxysilane was employed as a functionalizing agent for improving the performance of TiO ₂ .	Mass loss is not present, which is a limitation in this study.	[87]
Bismuth oxyiodide/TiO ₂	PVC	30.8% after 336 h	UV light	Photocatalytic solid-phase decomposition by BiOI/TiO ₂ worked under ambient conditions.	Too much time-consuming with very low degradation. Metal loading ratio effect on degradation performance	[81]
Ag-doped TiO ₂	Polythene film	14.28% after 300 h	UV light	The introduction of metal loading on TiO ₂ has the potential to decompose the plastics without secondary pollution production.		
Vitamin C modified TiO ₂	PVC film	71% after 216 h	UV light	The degradation rate was 2 times higher as compared to pure TiO ₂ and 15 times higher than PVC film.	The optimal vitamin C ratio was 0.5%, suggesting that the loading effect the plastic degradation rate.	[75]
FePcCl ₁₆ -TiO ₂	PVC film	81% after 15 days	UV light	FePcCl ₁₆ -TiO ₂ can work continually for 4 weeks.	A degradation pathway was not proposed. Only excited by UV radiation from solar light.	[93]
CuPc modified TiO ₂	PE	36% after 160 h	Solar light	CuPc modified TiO ₂ can produce more reactive oxygen species, and the optimal CuPc surface concentration was 0.3 monolayer on TiO ₂ .		
CuPc-TiO ₂	PS	6.9% after 250 h	Fluorescent lamp	Faster charge generation and separation both outside and inside the film surface.	The effect of CuPc loading on TiO ₂ needs further study. Bond breakage was limited under solar light.	[74]
FePc-TiO ₂	PS	35% after 250 h	Sunlight	Cleavage of the benzene ring is only observed under UV light.		
Amine Modified Aromatic Polyamide Dendrimer Modified TiO ₂	PS	19.89% after 600 h	Solar light	Catalyst has better dispersion ability in PS and an abundant number of amine groups at the periphery that absorb visible light.	Hard photodegradation under solar light due to a hindered amine.	[84]
Carbon coated TiO ₂	PP film	–	UV light	Bond scission, crosslinking, and decomposition of PP film affect the properties of the catalyst.	Mass loss % is not presented.	[100]
DMC modified TiO ₂	LDPE	68.38% after 400 h	UV light	An effective approach for LDPE degradation.	Weight loss is not effective under solar light.	[80]
Graphite doped TiO ₂	PVC	17.24% after 30 h	UV light	Graphite-doped TiO ₂ can effectively separate the charges.	Doping weight needs further study.	[90]
Grafted TiO ₂ Polyacrylamide grafted TiO ₂	PS PE	29% after 300 h 39.85% after 520 h	UV light	Cleavage of benzene ring under UV light. Improved hydrophilicity enhanced the degradation rate.	Only work under UV light. PE matrix absorbs moisture.	[91] [76]
TiO ₂	PS	22.5% after 150 h	UV light	The PS-TiO ₂ film showed efficient performance; diffusion of reactive species takes place on the TiO ₂ surface.	Limited degradation.	[101]
	PP	–	UV light		Weight loss % was not given.	[94]

(continued on next page)

Table 1 (continued)

Catalyst	Target Plastic	Degradation Efficiency	Light Source	Remark	Limitation	Reference
Poly(ethylene oxide) microcapsule containing TiO ₂				The suppression effect was raised due to the addition of phenolic antioxidants in the initial phase of PP decomposition.		
TiO ₂	PP film	8% after 144 h	Xenon lamp	Composite of the catalyst with plastic with different concentrations.	Insignificant degradation.	[102]
TiO ₂	HDPE	–	UV light	Anatase TiO ₂ slightly enhanced solar reflectance.	Weight loss % was not given.	[103]
Degussa P25 (TiO ₂)	polyamide 66	97%	UVC light	Decomposition performance was optimized with 100 mg TiO ₂ /L dose under UVC.	Work only under UVC system.	[104]
Ag/TiO ₂ /RGO	PE	76%	UV light	Modified TiO ₂ showed significant performance as compared to pure and Ag/TiO ₂ .	Catalyst slurry requires irradiation for 6 h which increases material cost and photocatalyst only works under UV light.	[105]
Nano-composite Ag/TiO ₂	PE	100%	UV light	Dopant addition displayed a good effect on PE decomposition.	Catalyst slurry requires irradiation for 6 h which increases material cost and photocatalyst only works under UV light.	[106]
Anodized TiO ₂	PS	23.5%	UV light	Ti foils with a missed structure including nanotubes and nano-grass decomposed the nano plastics PS.	Limited degradation efficiency.	[67]
TiO ₂ @amylose/polyiodide/hydroxyethyl cellulose	LDPE	15%	Xenon lamp	Catalyst exhibit tunable and self-indicating tardy onset of activity.	Costly methods for material preparation, require further study on reaction intermediates and their toxicity.	[107]

Note: This symbol “–” indicates that data is not present.

interests or personal relationships that could have appeared to influence the work reported in this paper.

Acknowledgments

The authors gratefully acknowledge support from National Natural Science Foundation of China (Nos. 21976030 and 22006020). The Natural Science Foundation of Shanghai (Nos. 19ZR1471200 and 17ZR1440200).

References

- [1] A.L. Andrade, M.A. Neal, Applications and societal benefits of plastics, *Philos. Trans. R. Soc. B Biol. Sci.* 364 (2009) 1977–1984, <https://doi.org/10.1098/rstb.2008.0304>.
- [2] M. Choudhary, C. Peter, S.K. Shukla, P.P. Govender, G.M. Joshi, R. Wang, Environmental issues: a challenge for wastewater treatment. *Green Materials for Wastewater Treatment*, Springer, 2020, pp. 1–12, https://doi.org/10.1007/978-3-030-17724-9_1.
- [3] Y. Chen, A.K. Awasthi, F. Wei, Q. Tan, J. Li, Single-use plastics: production, usage, disposal, and adverse impacts, *Sci. Total Environ.* (2020), 141772, <https://doi.org/10.1016/j.scitotenv.2020.141772>.
- [4] E.J. Carpenter, K.L. Smith, Plastics on the Sargasso Sea surface, *Science* 175 (1972) 1240–1241. (<https://doi.org/10.1126/science.175.4027.1240>).
- [5] J.A. Ivar do Sul, M.F. Costa, The present and future of microplastic pollution in the marine environment, *Environ. Pollut.* 185 (2014) 352–364, <https://doi.org/10.1016/j.envpol.2013.10.036>.
- [6] T.S.M. Amelia, W.M.A.W.M. Khalik, M.C. Ong, Y.T. Shao, H.-J. Pan, K. Bhubalan, Marine microplastics as vectors of major ocean pollutants and its hazards to the marine ecosystem and humans, *Prog. Earth Planet. Sci.* 8 (2021) 12, <https://doi.org/10.1186/s40645-020-00405-4>.
- [7] Y. Zhang, S. Kang, S. Allen, D. Allen, T. Gao, M. Sillanpää, Atmospheric microplastics: a review on current status and perspectives, *Earth Sci. Rev.* 203 (2020), 103118, <https://doi.org/10.1016/j.earscirev.2020.103118>.
- [8] L. Camarero, M. Bacardit, A. de Diego, G.J.A.E. Arana, Decadal trends in atmospheric deposition in a high elevation station: effects of climate and pollution on the long-range flux of metals and trace elements over SW Europe, *Atmos. Environ.* 167 (2017) 542–552, <https://doi.org/10.1016/j.atmosenv.2017.08.049>.
- [9] P.G. Ryan, C.J. Moore, J.A. van Franeker, C.L. Moloney, Monitoring the abundance of plastic debris in the marine environment, *Philos. Trans. R. Soc. B Biol. Sci.* 364 (2009) 1999–2012, <https://doi.org/10.1098/rstb.2008.0207>.
- [10] R.C. Thompson, S.H. Swan, C.J. Moore, F.S. Vom Saal, Our plastic age, *The Royal Society Publishing*, *Philos. Trans. R. Soc. Lond., B, Biol. Sci.*, 2009, <https://doi.org/10.1098/rstb.2009.0054>.
- [11] D.K. Barnes, F. Galgani, R.C. Thompson, M. Barlaz, Accumulation and fragmentation of plastic debris in global environments, *Philos. Trans. R. Soc. B Biol. Sci.* 364 (2009) 1985–1998, <https://doi.org/10.1098/rstb.2008.0205>.
- [12] C. Giacovelli, Single-use plastics: a roadmap for sustainability, (2018), (<https://stg-wedocs.unep.org/handle/20.500.11822/25496>).
- [13] D. Knoblauch, L. Mederake, U. Stein, Developing countries in the lead—what drives the diffusion of plastic bag policies? *Sustainability* 10 (2018) 1994, <https://doi.org/10.3390/su10061994>.
- [14] K. Hu, W. Tian, Y. Yang, G. Nie, P. Zhou, Y. Wang, X. Duan, S.J.W.R. Wang, Microplastics remediation in aqueous systems: strategies and technologies, *Water Res.* (2021), 117144, <https://doi.org/10.1016/j.watres.2021.117144>.
- [15] B. Gewert, M.M. Plassmann, M.J.E.S.P. MacLeod, Impacts, Pathways for degradation of plastic polymers floating in the marine environment, *Environ. Sci. Process. Impact.* 17 (2015) 1513–1521. (<https://doi.org/10.1039/C5EM00207A>).
- [16] J. Boucher, F. Faure, O. Pompini, Z. Plummer, O. Wieser, L.F. de Alencastro, (Micro) plastic fluxes and stocks in Lake Geneva basin, *TrAC Trends Anal. Chem.* 112 (2019) 66–74, <https://doi.org/10.1016/j.trac.2018.11.037>.
- [17] L. Wang, T. Lin, C. Yan, W. He, J. Wang, Q. Tang, Effects of different film residue and irrigation quota on nutrient and water use efficiency of cotton under drip irrigation, *J. Plant. Nutr.* 24 (2018) 122–133.
- [18] A.E. Cartraud, M. Le Corre, J. Turquet, J. Tourmetz, Plastic ingestion in seabirds of the western Indian Ocean, *Mar. Pollut. Bull.* 140 (2019) 308–314, <https://doi.org/10.1016/j.marpolbul.2019.01.065>.
- [19] M. Rizzi, F.L. Rodrigues, L. Medeiros, I. Ortega, L. Rodrigues, D.S. Monteiro, F. Kessler, M.C. Proietti, Ingestion of plastic marine litter by sea turtles in southern Brazil: abundance, characteristics and potential selectivity, *Mar. Pollut. Bull.* 140 (2019) 536–548, <https://doi.org/10.1016/j.marpolbul.2019.01.054>.
- [20] C.J. Moore, Synthetic polymers in the marine environment: a rapidly increasing, long-term threat, *Environ. Res.* 108 (2008) 131–139, <https://doi.org/10.1016/j.enrev.2008.07.025>.
- [21] S. Chatterjee, S. Sharma, Microplastics in our oceans and marine health, *Field Actions Sci. Rep.* (2019) 54–61. (<http://journals.openedition.org/factsreports/5257>).
- [22] R. Gillibert, G. Balakrishnan, Q. Deshoules, M. Tardivel, A. Magazzù, M. G. Donato, O.M. Marago, M. Lamy de La Chapelle, F. Colas, F. Lagarde, P. G. Gucciardi, Raman tweezers for small microplastics and nanoplastics identification in seawater, *Environ. Sci. Technol. Lett.* 53 (2019) 9003–9013, <https://doi.org/10.1021/acs.est.9b03105>.
- [23] M. Cai, H. He, M. Liu, S. Li, G. Tang, W. Wang, P. Huang, G. Wei, Y. Lin, B. Chen, Lost but can't be neglected: huge quantities of small microplastics hide in the South China Sea, *Sci. Total Environ.* 633 (2018) 1206–1216, <https://doi.org/10.1016/j.scitotenv.2018.03.197>.
- [24] L. Peng, D. Fu, H. Qi, C.Q. Lan, H. Yu, C. Ge, Micro- and nano-plastics in marine environment: source, distribution and threats - a review, *Sci. Total. Environ.* 698 (2020), 134254, <https://doi.org/10.1016/j.scitotenv.2019.134254>.
- [25] M. Lehtiniemi, S. Hartikainen, P. Näkki, J. Engström-Öst, A. Koistinen, O. Setälä, Size matters more than shape: ingestion of primary and secondary microplastics by small predators, *Food Webs* 17 (2018), e00097, <https://doi.org/10.1016/j.foodweb.2018.e00097>.

- [26] M.C. Rillig, R. Ingraffia, A.A. de Souza Machado, Microplastic incorporation into soil in agroecosystems, *Front. Plant Sci.* 8 (2017) 1805, <https://doi.org/10.3389/fpls.2017.01805>.
- [27] M.C. Borrás, R. Sluyter, P.J. Barker, K. Konstantinov, S. Bakand, Y_2O_3 decorated TiO_2 nanoparticles: enhanced UV attenuation and suppressed photocatalytic activity with promise for cosmetic and sunscreen applications, *J. Photochem. Photobiol. B Biol.* (2020), 111883, <https://doi.org/10.1016/j.jphotobiol.2020.111883>.
- [28] G.K. Upadhyay, V. Kumar, L. Purohit, Optimized CdO: TiO_2 nanocomposites for heterojunction solar cell applications, *J. Alloy. Compd.* (2020), 157453, <https://doi.org/10.1016/j.jallcom.2020.157453>.
- [29] V.V. Pillai, S.P. Lonkar, S.M. Alhassan, Template-free, solid-state synthesis of hierarchically macroporous S-doped TiO_2 nano-photocatalysts for efficient water remediation, *ACS Omega* 5 (2020) 7969–7978, <https://doi.org/10.1021/acsomega.9b04409>.
- [30] A. Azimzada, J.M. Farner, I. Jreije, M. Hadioui, C. Liu-Kang, N. Tufenkji, P. Shaw, K.J. Wilkinson, Single-and multi-element quantification and characterization of TiO_2 nanoparticles released from outdoor stains and paints, *Front. Environ. Sci.* (2020). (<https://doi.org/10.3389/fenvs.2020.00091>).
- [31] X. Wang, X. Li, X. Yang, K. Lei, L. Wang, The innovative fabrication of nano-natural antimicrobial agent@ polymeric microgels- TiO_2 hybrid films capable of absorbing UV and antibacterial on touch screen panel, *Colloids Surf. B Biointerfaces* (2020), 111410, <https://doi.org/10.1016/j.colsurfb.2020.111410>.
- [32] D.I. Tishkevich, A.I. Vorobjova, D.A. Vinnik, Template assisted Ni nanowires fabrication, *Mater. Sci. Forum* 946 (2019) 235–241, <https://doi.org/10.4028/www.scientific.net/MSF.946.235>.
- [33] A. Vorobjova, D. Tishkevich, D. Shimanovich, T. Zuban, K. Astapovich, A. Kozlovskiy, M. Zdrovets, A. Zhaludkevich, D. Lyakhov, D.J.R.A. Michels, The influence of the synthesis conditions on the magnetic behaviour of the densely packed arrays of Ni nanowires in porous anodic alumina membranes, *RSC Adv.* 11 (2021) 3952–3962, <https://doi.org/10.1039/DORA07529A>.
- [34] A.I. Vorobjova, D.L. Shimanovich, O.A. Sycheva, T.I. Ezovitova, D.I. Tishkevich, A.V. Trykhanov, Studying the thermodynamic properties of composite magnetic material based on anodic alumina, *Russ. Microelectron.* 48 (2019) 107–118, <https://doi.org/10.1134/S1063739719020100>.
- [35] A. Vorobjova, D. Tishkevich, D. Shimanovich, M. Zdrovets, A. Kozlovskiy, T. Zuban, D. Vinnik, M. Dong, S. Trukhanov, A. Trukhanov, V. Fedosyuk, Electrochemical behaviour of $\text{Ti}/\text{Al}_2\text{O}_3/\text{Ni}$ nanocomposite material in artificial physiological solution: prospects for biomedical application, *Nanomaterials* 10 (2020), <https://doi.org/10.3390/nano10010173>.
- [36] D.I. Tishkevich, S.S. Grabchikov, S.B. Lastovskii, S.V. Trukhanov, T.I. Zuban, D. S. Vasin, A.V. Trukhanov, A.L. Kozlovskiy, M.M. Zdrovets, Effect of the synthesis conditions and microstructure for highly effective electron shields production based on Bi coatings, *ACS Appl. Energy Mater.* 1 (2018) 1695–1702, <https://doi.org/10.1021/acsami.8b00179>.
- [37] A.-U.-R. Bacha, H. Cheng, J. Han, I. Nabi, K. Li, T. Wang, Y. Yang, S. Ajmal, Y. Liu, L. Zhang, Significantly accelerated PEC degradation of organic pollutant with addition of sulfite and mechanism study, *Appl. Catal. B Environ.* 248 (2019) 441–449, <https://doi.org/10.1016/j.apcatb.2019.02.049>.
- [38] A.-U.-R. Bacha, I. Nabi, Z. Fu, K. Li, H. Cheng, L. Zhang, A comparative study of bismuth-based photocatalysts with titanium dioxide for perfluorooctanoic acid degradation, *Chin. Chem. Lett.* 30 (2019) 2225–2230, <https://doi.org/10.1016/j.clet.2019.07.058>.
- [39] A.-U.-R. Bacha, I. Nabi, H. Cheng, K. Li, S. Ajmal, T. Wang, L. Zhang, Photocatalytic degradation of endocrine-disruptor bisphenol-A with significantly activated peroxyxonosulfate by Co-BiVO₄ photoanode, *Chem. Eng. J.* 389 (2020), <https://doi.org/10.1016/j.cej.2020.124482>.
- [40] J. Moma, J.J.P.-A. Baloyi, Attributes, Modified titanium dioxide for photocatalytic applications, *Photocatal. Appl. Attrib.* 18 (2019). (<https://doi.org/10.5772/intechopen.79374>).
- [41] M. Skocaj, M. Filipic, J. Petkovic, S. Novak, Titanium dioxide in our everyday life; is it safe? *Radiol. Oncol.* 45 (2011) 227–247. (<https://doi.org/10.2478/v10019-011-0037-0>).
- [42] C.H.A. Tsang, K. Li, Y. Zeng, W. Zhao, T. Zhang, Y. Zhan, R. Xie, D.Y.C. Leung, H. Huang, Titanium oxide based photocatalytic materials development and their role of in the air pollutants degradation: overview and forecast, *Environ. Int.* 125 (2019) 200–228, <https://doi.org/10.1016/j.envint.2019.01.015>.
- [43] X. Hu, G. Li, J.C. Yu, Design, fabrication, and modification of nanostructured semiconductor materials for environmental and energy applications, *Langmuir* 26 (2010) 3031–3039, <https://doi.org/10.1021/la902142b>.
- [44] S. Malato, J. Blanco, A. Vidal, C. Richter, Photocatalysis with solar energy at a pilot-plant scale: an overview, *Appl. Catal. B Environ.* 37 (2002) 1–15, [https://doi.org/10.1016/S0926-3373\(01\)00315-0](https://doi.org/10.1016/S0926-3373(01)00315-0).
- [45] S.N.A. Shah, Z. Shah, M. Hussain, M. Khan, Hazardous effects of titanium dioxide nanoparticle in ecosystem, *Bioinorg. Chem. Appl.* 2017 (2017), 4101735, <https://doi.org/10.1155/2017/4101735>.
- [46] K. Hashimoto, H. Irie, A. Fujishima, TiO_2 photocatalysis: a historical overview and future prospects, *Jpn. J. Appl. Phys.* 44 (2005) 8269, <https://doi.org/10.1143/JJAP.44.8269>.
- [47] B. Wang, G.-Y. Cui, B.-B. Zhang, Z. Li, H.-X. Ma, W. Wang, F.-Y. Zhang, X.-X. Ma, Novel axial substituted subphthalocyanine and its TiO_2 photocatalyst for degradation of organic water pollutant under visible light, *Opt. Mater.* 109 (2020), 110202, <https://doi.org/10.1016/j.optmat.2020.110202>.
- [48] M. Peñas-Garzón, A. Gómez-Avilés, C. Belver, J. Rodríguez, J. Bedía, Degradation pathways of emerging contaminants using TiO_2 -activated carbon heterostructures in aqueous solution under simulated solar light, *Chem. Eng. J.* (2020), 124867, <https://doi.org/10.1016/j.cej.2020.124867>.
- [49] M.C. Ariza-Tarazona, J.F. Villarreal-Chiu, V. Barbieri, C. Siligardi, E.I. Cedillo-González, New strategy for microplastic degradation: green photocatalysis using a protein-based porous N- TiO_2 semiconductor, *Ceram. Int.* 45 (2019) 9618–9624, <https://doi.org/10.1016/j.ceramint.2018.10.208>.
- [50] L. Li, The reaction mechanism of photoelectrocatalysis on the surface of TiO_2 nanotube array electrode, *Asia-Pac. J. Chem. Eng.* (2020) e2511, <https://doi.org/10.1002/apj.2511>.
- [51] U. Martinez, B. Hammer, Adsorption properties versus oxidation states of rutile TiO_2 (110), *J. Chem. Phys.* 134 (2011), 194703, <https://doi.org/10.1063/1.3589861>.
- [52] M. Pawar, S. Topcu Sendogdu, P. Gouma, A brief overview of TiO_2 photocatalyst for organic dye remediation: case study of reaction mechanisms involved in Ce- TiO_2 photocatalysts system, *J. Nanomat.* 2018 (2018), 5953609, <https://doi.org/10.1155/2018/5953609>.
- [53] X. He, A. Wang, P. Wu, S. Tang, Y. Zhang, L. Li, P. Ding, Photocatalytic degradation of microcystin-LR by modified TiO_2 photocatalysis: a review, *Sci. Total. Environ.* 743 (2020), 140694, <https://doi.org/10.1016/j.scitotenv.2020.140694>.
- [54] S. Gligorovski, R. Strelkowski, S. Barbat, D. Vione, Environmental implications of hydroxyl radicals ($\bullet\text{OH}$), *Chem. Rev.* 115 (2015) 13051–13092, <https://doi.org/10.1021/cr500310b>.
- [55] A.D. Proctor, B.M. Bartlett, Hydroxyl radical suppression during photoelectrocatalytic water oxidation on WO_3/FeOOH , *J. Phys. Chem. C* 124 (2020) 17957–17963, <https://doi.org/10.1021/acs.jpcc.0c04820>.
- [56] K. Santhi, M. Navaneethan, S. Harish, S. Ponnamy, C. Muthamizhchelvan, Synthesis and characterization of TiO_2 nanorods by hydrothermal method with different pH conditions and their photocatalytic activity, *Appl. Surf. Sci.* 500 (2020), 144058, <https://doi.org/10.1016/j.apsusc.2019.144058>.
- [57] P.S. Basavarajappa, S.B. Patil, N. Ganganaappa, K.R. Reddy, A.V. Raghu, C. V. Reddy, Recent progress in metal-doped TiO_2 , non-metal doped/codoped TiO_2 and TiO_2 nanostructured hybrids for enhanced photocatalysis, *Int. J. Hydr. Energy* 45 (2020) 7764–7778, <https://doi.org/10.1016/j.ijhydene.2019.07.241>.
- [58] Z. Ma, Q. Jia, C. Tao, B. Han, Highlighting unique function of immobilized superoxide on TiO_2 for selective photocatalytic degradation, *Sep. Purif. Technol.* 238 (2020), 116402, <https://doi.org/10.1016/j.seppur.2019.116402>.
- [59] A. Ajmal, I. Majeed, R.N. Malik, H. Idriess, M.A. Nadeem, Principles and mechanisms of photocatalytic dye degradation on TiO_2 based photocatalysts: a comparative overview, *RSC Adv.* 4 (2014) 37003–37026, <https://doi.org/10.1039/C4RA06658H>.
- [60] C. Galindo, P. Jacques, A. Kalt, Photodegradation of the aminoazobenzene acid orange 52 by three advanced oxidation processes: UV/ H_2O_2 , UV/ TiO_2 and VIS/ TiO_2 : comparative mechanistic and kinetic investigations, *J. Photochem. Photobiol. A Chem.* 130 (2000) 35–47, [https://doi.org/10.1016/S1010-6030\(99\)00199-9](https://doi.org/10.1016/S1010-6030(99)00199-9).
- [61] Y. Ma, J.-Y. Yao, Photodegradation of Rhodamine B catalyzed by TiO_2 thin films, *J. Photochem. Photobiol. A Chem.* 116 (1998) 167–170, [https://doi.org/10.1016/S1010-6030\(98\)00295-0](https://doi.org/10.1016/S1010-6030(98)00295-0).
- [62] I.A. Neacșu, A.I. Nicoară, O.R. Vasile, B.Ş. Vasile, Chapter 9 - Inorganic micro- and nanostructured implants for tissue engineering, in: A.M. Grumezescu (Ed.), *Nanobiomaterials in Hard Tissue Engineering*, William Andrew Publishing, 2016, pp. 271–295, <https://doi.org/10.1016/B978-0-323-42862-0-00009-2>.
- [63] E. Yilmaz, M. Soylak, 15 - Functionalized nanomaterials for sample preparation methods, in: C. Mustansar Hussain (Ed.), *Handbook of Nanomaterials in Analytical Chemistry*, Elsevier, 2020, pp. 375–413, <https://doi.org/10.1016/B978-0-12-816699-4-00015-3>.
- [64] M. Romero Saez, L. Jaramillo, R. Saravanan, N. Benito, E. Pabón, E. Mosquera, F. Gracia Caroca, Notable photocatalytic activity of TiO_2 -polyethylene nanocomposites for visible light degradation of organic pollutants, *Polym. Lett.* (2017). (<https://doi.org/10.3144/expresspolymlett.2017.86>).
- [65] S. Li, S. Xu, L. He, F. Xu, Y. Wang, L. Zhang, Photocatalytic degradation of polyethylene plastic with polypyrrole/ TiO_2 nanocomposite as photocatalyst, *Polym. Plast. Technol. Eng.* 49 (2010) 400–406, <https://doi.org/10.1080/03602550903532166>.
- [66] R.T. Thomas, V. Nair, N. Sandhyarani, TiO_2 nanoparticle assisted solid phase photocatalytic degradation of polythene film: a mechanistic investigation, *Colloids Surf. A Physicochem. Eng. Asp.* 422 (2013) 1–9, <https://doi.org/10.1016/j.colsurfa.2013.01.017>.
- [67] L.P. Domínguez-Jaimes, E.I. Cedillo-González, E. Luévano-Hipólito, J.D. Acuña-Bedoya, J.M. Hernández-López, Degradation of primary nanoplastics by photocatalysis using different anodized TiO_2 structures, *J. Hazard. Mater.* 413 (2021), 125452, <https://doi.org/10.1016/j.jhazmat.2021.125452>.
- [68] Y. Liu, D. Zhu, Chapter 8 - Asymmetrical phthalocyanines, in: H.S. Nalwa (Ed.), *Handbook of Surfaces and Interfaces of Materials*, Academic Press, Burlington, 2001, pp. 405–438, <https://doi.org/10.1016/B978-012513910-6/50054-2>.
- [69] D. Eley, Phthalocyanines as semiconductors, *Nature* 162 (1948), <https://doi.org/10.1038/162819a0> (819–819).
- [70] P.-C. Lo, M.S. Rodríguez-Morgade, R.K. Pandey, D.K. Ng, T. Torres, F. Dumoulin, The unique features and promises of phthalocyanines as advanced photosensitisers for photodynamic therapy of cancer, *Chem. Soc. Rev.* 49 (2020) 1041–1056, <https://doi.org/10.1039/C9CS00129H>.
- [71] D. Gounden, N. Nombona, W.E. van Zyl, Recent advances in phthalocyanines for chemical sensor, non-linear optics (NLO) and energy storage applications, *Coord. Chem. Rev.* 420 (2020), 213359, <https://doi.org/10.1016/j.ccr.2020.213359>.

- [72] W. Fa, L. Zan, C. Gong, J. Zhong, K. Deng, Solid-phase photocatalytic degradation of polystyrene with TiO₂ modified by iron (II) phthalocyanine, *Appl. Catal. B Environ.* 79 (2008) 216–223, <https://doi.org/10.1016/j.apcatb.2007.10.018>.
- [73] X. Zhao, Z. Li, Y. Chen, L. Shi, Y. Zhu, Enhancement of photocatalytic degradation of polyethylene plastic with CuPc modified TiO₂ photocatalyst under solar light irradiation, *Appl. Surf. Sci.* 254 (2008) 1825–1829, <https://doi.org/10.1016/j.apusc.2007.07.154>.
- [74] J. Shang, M. Chai, Y. Zhu, Photocatalytic degradation of polystyrene plastic under fluorescent light, *Environ. Sci. Technol.* 37 (2003) 4494–4499, <https://doi.org/10.1021/es0209464>.
- [75] C. Yang, C. Gong, T. Peng, K. Deng, L. Zan, High photocatalytic degradation activity of the polyvinyl chloride (PVC)-vitamin C (VC)-TiO₂ nano-composite film, *J. Hazard. Mater.* 178 (2010) 152–156, <https://doi.org/10.1016/j.jhazmat.2010.01.056>.
- [76] W. Liang, Y. Luo, S. Song, X. Dong, X. Yu, High photocatalytic degradation activity of polyethylene containing polyacrylamide grafted TiO₂, *Polym. Degrad. Stab.* 98 (2013) 1754–1761, <https://doi.org/10.1016/j.polymdegradstab.2013.05.027>.
- [77] B.E. Llorente-García, J.M. Hernández-López, A.A. Zaldívar-Cadena, C. Siligardi, E.I. Cedillo-González, First insights into photocatalytic degradation of HDPE and LDPE microplastics by a mesoporous N-TiO₂ coating: effect of size and shape of microplastics, *Coatings* 10 (2020), <https://doi.org/10.3390/coatings10070658>.
- [78] C. Yang, L. Tian, L. Ye, T. Peng, K. Deng, L. Zan, Enhancement of photocatalytic degradation activity of poly (vinyl chloride)-TiO₂ nanocomposite film with polyoxometalate, *J. Appl. Polym. Sci.* 120 (2011) 2048–2053, <https://doi.org/10.1002/app.33316>.
- [79] W. Mekprasart, T. Thongpradith, W. Pecharapa, K.N. Ishihara, Photocatalytic properties and plastic degradation of TiO₂ nanocomposite with synthetic-rutile from natural ore, *J. Japan Soc. Powder Metall.* 65 (2018) 719–724, <https://doi.org/10.2497/jjspm.65.719>.
- [80] L. Zan, W. Fa, S. Wang, Novel photodegradable low-density polyethylene–TiO₂ nanocomposite film, *Environ. Sci. Technol.* 40 (2006) 1681–1685, <https://doi.org/10.1021/es051173x>.
- [81] C. Yang, K. Deng, T. Peng, L. Zan, Enhanced solid-phase photocatalytic degradation activity of a poly(vinyl chloride)-TiO₂ nanocomposite film with bismuth oxyiodide, *Chem. Eng. Technol.* 34 (2011) 886–892, <https://doi.org/10.1002/ceat.201000450>.
- [82] W. Fa, L. Guo, J. Wang, R. Guo, Z. Zheng, F. Yang, Solid-phase photocatalytic degradation of polystyrene with TiO₂/Fe(St)₃ as catalyst, *J. Appl. Polym. Sci.* 128 (2013) 2618–2622, <https://doi.org/10.1002/app.37751>.
- [83] R. Verma, S. Singh, M. Dalai, M. Saravanan, V.V. Agrawal, A.K.J.M. Srivastava, Design, Photocatalytic degradation of polypropylene film using TiO₂-based nanomaterials under solar irradiation, *Mater. Des.* 133 (2017) 10–18, <https://doi.org/10.1016/j.matdes.2017.07.042>.
- [84] Y. Lei, H. Lei, J. Huo, Innovative controllable photocatalytic degradation of polystyrene with hindered amine modified aromatic polyamide dendrimer/polystyrene-grafted-TiO₂ photocatalyst under solar light irradiation, *Polym. Degrad. Stab.* 118 (2015) 1–9, <https://doi.org/10.1016/j.polymdegradstab.2015.04.005>.
- [85] T. Soitong, Photo-degradation of polypropylene-ascorbic acid TiO₂ composite films, *Int. Polym. Process.* 33 (2018) 29–34, <https://doi.org/10.3139/217.3315>.
- [86] I. Nabi, A.U. Bacha, K. Li, H. Cheng, T. Wang, Y. Liu, S. Ajmal, Y. Yang, Y. Feng, L. Zhang, Complete photocatalytic mineralization of microplastic on TiO₂ nanoparticle film, *iScience* 23 (2020), 101326, <https://doi.org/10.1016/j.isci.2020.101326>.
- [87] J. Alvarado, G. Acosta, F. Perez, Study of the effect of the dispersion of functionalized nanoparticles TiO₂ with photocatalytic activity in LDPE, *Polym. Degrad. Stab.* 134 (2016) 376–382, <https://doi.org/10.1016/j.polymdegradstab.2016.11.009>.
- [88] P. Peerakiatkajohn, W. Onreabroy, C. Chawengkijwanich, S. Chiarakorn, Preparation of visible-light-responsive TiO₂ doped Ag thin film on PET plastic for BTEX treatment, *J. Sustain. Energy Environ.* 2 (2011) 121–125.
- [89] M.C. Ariza-Tarazona, J.F. Villarreal-Chiu, J.M. Hernandez-Lopez, J. Rivera De la Rosa, V. Barbieri, C. Siligardi, E.I. Cedillo-Gonzalez, Microplastic pollution reduction by a carbon and nitrogen-doped TiO₂: effect of pH and temperature in the photocatalytic degradation process, *J. Hazard. Mater.* 395 (2020), 122632, <https://doi.org/10.1016/j.jhazmat.2020.122632>.
- [90] Y. Zhang, T. Sun, D. Zhang, Z. Shi, X. Zhang, C. Li, L. Wang, J. Song, Q. Lin, Enhanced photodegradability of PVC plastics film by codoping nano-graphite and TiO₂, *Polym. Degrad. Stab.* 181 (2020), <https://doi.org/10.1016/j.polymdegradstab.2020.109332>.
- [91] L. Zan, L. Tian, Z. Liu, Z. Peng, A new polystyrene-TiO₂ nanocomposite film and its photocatalytic degradation, *Appl. Catal. A Gen.* 264 (2004) 237–242, <https://doi.org/10.1016/j.apcata.2003.12.046>.
- [92] Y. An, J. Hou, Z. Liu, B. Peng, Enhanced solid-phase photocatalytic degradation of polyethylene by TiO₂-MWCNTs nanocomposites, *Mater. Chem. Phys.* 148 (2014) 387–394, <https://doi.org/10.1016/j.matchemphys.2014.08.001>.
- [93] W. Fa, C. Gong, L. Tian, T. Peng, L. Zan, Enhancement of photocatalytic degradation of poly(vinyl chloride) with perchlorinated iron (II) phthalocyanine modified nano-TiO₂, *J. Appl. Polym. Sci.* 122 (2011) 1823–1828, <https://doi.org/10.1002/app.34230>.
- [94] K. Miyazaki, H. Nakatani, Preparation of degradable polypropylene by an addition of poly(ethylene oxide) microcapsule containing TiO₂, *Polym. Degrad. Stab.* 94 (2009) 2114–2120, <https://doi.org/10.1016/j.polymdegradstab.2009.10.001>.
- [95] F. Miao, Y. Liu, M. Gao, X. Yu, P. Xiao, M. Wang, S. Wang, X. Wang, Degradation of polyvinyl chloride microplastics via an electro-Fenton-like system with a TiO₂/graphite cathode, *J. Hazard. Mater.* 399 (2020), 123023, <https://doi.org/10.1016/j.jhazmat.2020.123023>.
- [96] W. Asghar, I.A. Qazi, H. Ilyas, A.A. Khan, M.A. Awan, M. Rizwan Aslam, Comparative solid phase photocatalytic degradation of polythene films with doped and undoped TiO₂ nanoparticles, *J. Nanomater.* 2011 (2011), <https://doi.org/10.1155/2011/461930>.
- [97] N. Sehlotho, T. Nyokong, Catalytic activity of iron and cobalt phthalocyanine complexes towards the oxidation of cyclohexene using tert-butylhydroperoxide and chloroperoxybenzoic acid, *J. Mol. Catal. A Chem.* 209 (2004) 51–57, <https://doi.org/10.1016/j.molcata.2003.08.014>.
- [98] R.T. Thomas, N. Sandhyarani, Enhancement in the photocatalytic degradation of low density polyethylene-TiO₂ nanocomposite films under solar irradiation, *RSC Adv.* 3 (2013) 14080–14087, <https://doi.org/10.1039/C3RA42226G>.
- [99] S. Horikoshi, N. Serpone, Y. Hisamatsu, H. Hidaka, Photocatalyzed degradation of polymers in aqueous semiconductor suspensions. 3. Photooxidation of a solid polymer: TiO₂-blended poly (vinyl chloride) film, *Environ. Sci. Technol.* 32 (1998) 4010–4016, <https://doi.org/10.1021/es9710464>.
- [100] M.M. Kamrannejad, A. Hasanzadeh, N. Nosoudi, L. Mai, A.A. Babaloo, Photocatalytic degradation of polypropylene/TiO₂ nano-composites, *Mater. Res. Bull.* 17 (2014) 1039–1046, <https://doi:10.1590/1516-1439.267214>.
- [101] J. Shang, M. Chai, Y. Zhu, Solid-phase photocatalytic degradation of polystyrene plastic with TiO₂ as photocatalyst, *J. Solid State Chem.* 174 (2003) 104–110, [https://doi.org/10.1016/S0022-4596\(03\)00183-X](https://doi.org/10.1016/S0022-4596(03)00183-X).
- [102] X. García-Montelongo, A. Martínez-De La Cruz, S. Vázquez-Rodríguez, L. M. Torres-Martínez, Photo-oxidative degradation of TiO₂/polypropylene films, *Mater. Res. Bull.* 51 (2014) 56–62, <https://doi.org/10.1016/j.materresbull.2013.11.040>.
- [103] S. Wang, J. Zhang, L. Liu, F. Yang, Y. Zhang, Evaluation of cooling property of high density polyethylene (HDPE)/titanium dioxide (TiO₂) composites after accelerated ultraviolet (UV) irradiation, *Sol. Energy Mater. Sol. Cells* 143 (2015) 120–127, <https://doi.org/10.1016/j.solmat.2015.06.032>.
- [104] J.-M. Lee, R. Busquets, I.-C. Choi, S.-H. Lee, J.-K. Kim, L.C. Campos, Photocatalytic degradation of polyamide 66; evaluating the feasibility of photocatalysis as a microfibre-targeting technology, *Water* 12 (2020), <https://doi.org/10.3390/w12123551>.
- [105] M.H. Fadli, M. Ibadurrohman, S. Slamet, Microplastic pollutant degradation in water using modified TiO₂ photocatalyst under UV-irradiation. IOP Conf. Ser. Mater. Sci. Eng., IOP Publishing, 2021, <https://doi.org/10.1088/1757-899X/1011/1/012055>.
- [106] D.A. Maulana, M. Ibadurrohman, Synthesis of nano-composite Ag/TiO₂ for polyethylene microplastic degradation applications. IOP Conf. Ser. Mater. Sci. Eng., IOP Publishing, 2021, <https://doi.org/10.1088/1757-899X/1011/1/012054>.
- [107] Y. Zhao, F. Zhang, J. Zhang, K. Zou, J. Zhang, C. Chen, M. Long, Q. Zhang, J. Wang, C. Zheng, Preparation of composite photocatalyst with tunable and self-indicating delayed onset of performance and its application in polyethylene degradation, *Appl. Catal. B Environ.* 286 (2021), 119918, <https://doi.org/10.1016/j.apcatb.2021.119918>.